Gastroenterology 2023;165:733–745

A Medium-Chain Fatty Acid Analogue Prevents Intestinal Failure–Associated Liver Disease in Preterm Yorkshire Piglets

Scott C. Fligor,[1,2] Savas T. Tsikis,[1,2] Thomas I. Hirsch,[1,2] Amy Pan,[1] Kamila Moskowitzova,[1,2] Lorena Rincon-Cruz,[1,2] Ashlyn E. Whitlock,[1,2] Paul D. Mitchell,[3] Arthur P. Nedder,[4] Kathleen M. Gura,[2,5] David A. Fraser,[6] and Mark Puder[1,2]

[1]*Vascular Biology Program, Department of Surgery, Boston Children's Hospital, Boston, Massachusetts;* [2]*Harvard Medical School, Boston, Massachusetts;* [3]*Institutional Centers for Clinical and Translational Research, Boston Children's Hospital, Boston, Massachusetts;* [4]*Animal Resources Children's Hospital, Boston Children's Hospital, Boston, Massachusetts;* [5]*Department of Pharmacy and the Division of Gastroenterology, Hepatology, and Nutrition, Boston Children's Hospital, Boston, Massachusetts; and* [6]*NorthSea Therapeutics, Amsterdam, Netherlands*

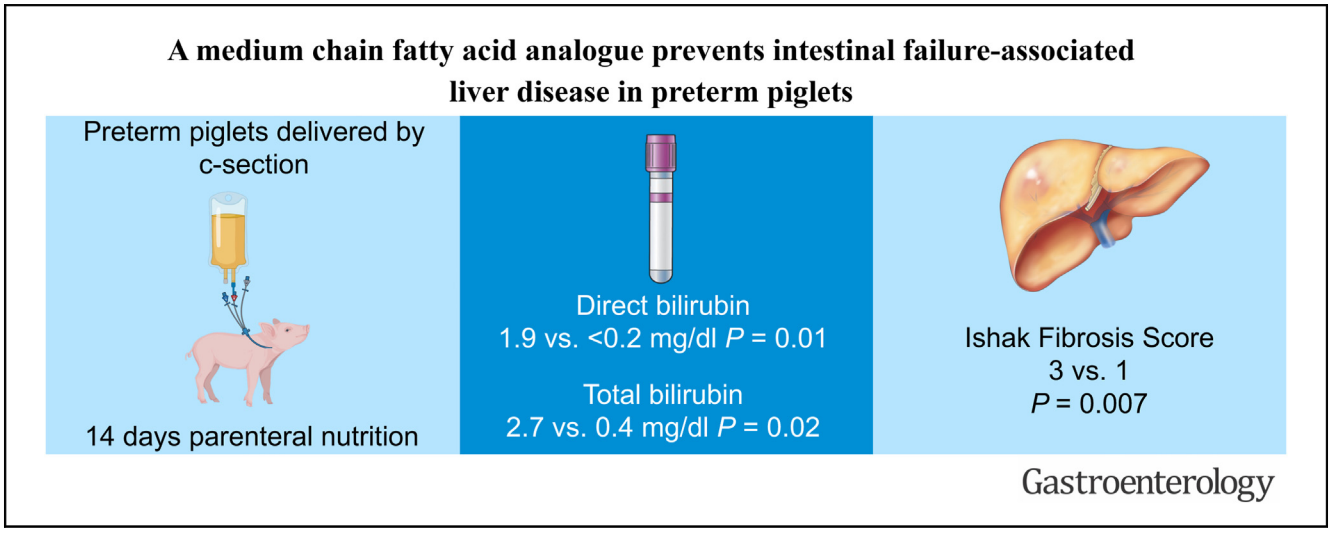

BACKGROUND & AIMS: At least 20%–30% of patients with intestinal failure receiving long-term parenteral nutrition will develop intestinal failure–associated liver disease (IFALD), for which there are few therapeutic options. SEFA-6179 is a first-in-class structurally engineered medium-chain fatty acid analogue that acts through GPR84, PPARα, and PPARγ agonism. We hypothesized that SEFA-6179 would prevent biochemical and histologic liver injury in a preterm piglet model of IFALD. **METHODS:** Preterm Yorkshire piglets were delivered by cesarean section, and parenteral nutrition was provided for 14 days via implanted central venous catheters. Animals were treated with either medium-chain triglyceride vehicle control or SEFA-6179. **RESULTS:** Compared to medium-chain triglyceride vehicle at day of life 15, SEFA-6179 prevented biochemical cholestasis (direct bilirubin: 1.9 vs <0.2 mg/dL, $P = .01$; total bilirubin: 2.7 vs 0.4 mg/dL, $P = .02$; gamma glutamyl transferase: 172 vs 30 U/L, $P = .01$). SEFA-6179 also prevented steatosis (45.6 vs 13.9 mg triglycerides/g liver tissue, $P = .009$), reduced bile duct proliferation (1.6% vs 0.5% area cytokeratin 7 positive, $P = .009$), and reduced fibrosis assessed by a masked pathologist (median Ishak score: 3 vs 1, $P = 0.007$). RNA sequencing of liver tissue demonstrated that SEFA-6179 broadly impacted inflammatory, metabolic, and fibrotic pathways, consistent with its in vitro receptor activity (GPR84/PPARα/PPARγ agonist). **CONCLUSIONS:** In a preterm piglet model of IFALD, SEFA-6179 treatment prevented biochemical cholestasis and steatosis and reduced bile duct proliferation and fibrosis. SEFA-6179 is a promising first-in-class therapy for the prevention and treatment of IFALD that will be investigated in an upcoming phase II clinical trial.

Keywords: Parenteral Nutrition; Cholestasis; Liver Diseases/Drug Therapy; Intestinal Failure; Models; Animal.

Parenteral nutrition is lifesaving for patients who cannot absorb sufficient nutrition and fluids through the gastrointestinal tract. However, long-term parenteral

Abbreviations used in this paper: **αSMA, α smooth muscle actin; ANCOVA, analysis of covariance; AUC, area under the curve; DOL, day of life; GO, Gene Ontology; GPR, G protein–coupled receptor; GPR84, G protein–coupled receptor 84; IFALD, intestinal failure–associated liver disease; IL, interleukin; IPA, Ingenuity Pathway Analysis; JNK, c-Jun N-terminal kinase; KEGG, Kyoto Encyclopedia of Genes and Genomes; LPS, lipopolysaccharide; MCFA, medium-chain fatty acid; MCT, medium-chain triglycerides; NF-κB, nuclear factor κB; PPARα, peroxisome proliferator-activated receptor α; PPARγ, peroxisome proliferator-activated receptor γ; RNA-Seq, RNA sequencing; RXR, retinoid X receptor; STAT3, signal transducer and activator of transcription 3; TGF-β, transforming growth factor β; TLR4, Toll-like receptor 4; TPN, total parenteral nutrition.**

Most current article

0016-5085
https://doi.org/10.1053/j.gastro.2023.05.035

HEPATOBILIARY

WHAT YOU NEED TO KNOW

BACKGROUND AND CONTEXT

Long-term parenteral nutrition in patients with intestinal failure often results in intestinal failure-associated liver disease (IFALD). SEFA-6179 is a medium-chain fatty acid analogue under development for IFALD.

NEW FINDINGS

In a preterm piglet model of IFALD, SEFA-6179 treatment prevented biochemical cholestasis and hepatosteatosis while reducing liver fibrosis. RNA sequencing demonstrated that SEFA-6179 broadly affected inflammatory, metabolic, and fibrotic pathways.

LIMITATIONS

The preterm piglet model is highly analogous to the preterm human infant with cholestatic IFALD, but older children and adults often have noncholestatic liver disease.

CLINICAL RESEARCH RELEVANCE

IFALD is a common complication of long-term parenteral nutrition in patients with intestinal failure, for whom there are few therapeutic options. SEFA-6179 is a promising first-in-class therapy for the prevention and treatment of IFALD that will be investigated in an upcoming phase 2 clinical trial.

BASIC RESEARCH RELEVANCE

SEFA-6179 is a first-in-class GPR84/PPARα/PPARγ agonist that targets inflammatory, metabolic, and fibrotic pathways. The unique mechanism of action of SEFA-6179 may provide a new avenue of investigation for other cholestatic liver diseases with limited therapeutic options.

nutrition can result in progressive cholestatic liver disease known as intestinal failure–associated liver disease (IFALD).[1,2] Premature neonates are at particularly high risk because of an immature liver poorly able to handle oxidative stress and inflammation, which is compounded by frequent sepsis and surgical gastrointestinal conditions such as necrotizing enterocolitis.[3]

The number of patients with intestinal failure surviving years or decades has increased markedly in recent years as advances in management have transitioned IFALD into a chronic liver disease.[4–6] For pediatric patients requiring long-term parenteral nutrition, persistently elevated liver enzymes and abnormal liver histology are common findings, particularly in patients for whom enteral autonomy is not achieved.[7–9] The long-term consequences of these abnormalities are unknown. There remains an urgent need for the development of new therapeutics for the prevention and treatment of IFALD.

Medium-chain fatty acids (MCFAs) are easily absorbed from the gastrointestinal tract into the portal circulation and, thus, are often used for nutritional support—in the form of medium-chain triglycerides (MCT)—for patients with impaired gastrointestinal absorption.[10] As a potential therapeutic, MCFAs are established ligands for G protein–coupled receptors (GPRs) and nuclear receptors that regulate metabolism, inflammation, and fibrogenesis, including GPR84, peroxisome proliferator-activated receptor α (PPARα), and peroxisome proliferator-activated receptor γ (PPARγ).[11–13] However, MCFA's rapid "glucose-like" metabolism, in combination with relatively low affinity and micromolar potency toward their established receptors, likely limits the utility of MCFAs as oral drugs in an unmodified form.[14] SEFA-6179 is an orally administered MCFA analogue that is designed to resist β-oxidation for use as a fuel source and achieve in vivo concentrations necessary for engagement of the aforementioned MCFA receptors. Here, we use a preterm piglet model of IFALD to investigate whether SEFA-6179 prevents biochemical and histologic IFALD.

Materials and Methods

Experimental Design

The aim of the study was to determine whether SEFA-6179 prevented biochemical cholestasis and histologic liver disease in a preterm piglet model of IFALD compared to MCT vehicle control. Previous studies have evaluated the preterm piglet model of IFALD and demonstrated biochemical cholestasis, similar to active IFALD seen in human neonates before the progression of steatotic-fibrotic liver disease.[15,16] Thus, the prespecified primary outcome assessed was plasma total and direct bilirubin. Secondary outcomes of interest included nutritional markers (weight, albumin), other biochemical markers of cholestasis (total bilirubin, gamma glutamyl transferase, plasma bile acids), steatosis (both histology and tissue triglyceride content), and fibrosis (Ishak fibrosis score).

All procedures were approved by the Boston Children's Hospital Institutional Animal Care and Use Committee and were conducted in accordance with the *Guide for the Care and Use of Laboratory Animals*.[17] ARRIVE (Animal Research: Reporting of In Vivo Experiments) guidelines were followed for reporting. The study design is shown in Figure 1. A pregnant Yorkshire sow (*Sus scrofa domesticus*) was obtained (Parson's Farm) and housed in our facility 5 days before cesarean section. Piglets were delivered at 5 days before full term (111-day gestation) via cesarean section. After resuscitation, single-lumen (3 Fr $\times$ 8 cm) central venous catheters (Cook Medical) were placed. Detailed procedural information is provided in the Supplementary Material.

Parenteral Nutrition

Total parenteral nutrition (TPN) was initiated on day of life (DOL) 1, advanced to goal over 5 days, and continued until sacrifice on DOL 15. The goal daily volume was 162 mL/kg/d; dextrose, 16 g/kg/d; amino acids, 9 g/kg/d; fat, 5.7 g/kg/d; and caloric content, 143 kcal/kg/d. The TPN composition was based on previously published work, with the volume decreased after the pilot cohort demonstrated intolerance of a higher dextrose infusion rate (see Supplementary Figure 1).[15] TPN was compounded daily. All intravenous tubing, including inline 1.2-μm air-eliminating filters (B. Braun), was changed daily. Detailed compounding and advancement information is provided in the Supplementary Material.

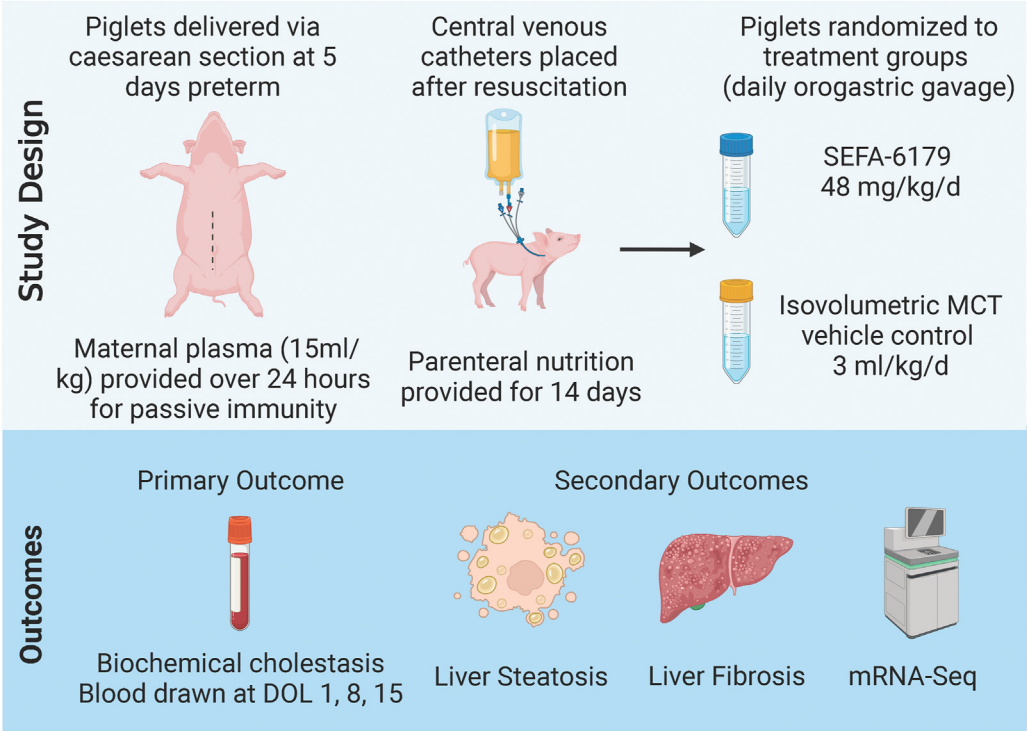

Figure 1. Study design. Figure created with Biorender.com. MCT, medium-chain triglyceride; mRNA, messenger RNA.

Group Allocation

After placement of central venous catheters on DOL 1, piglets were allocated into the treatment group (SEFA-6179) or control group (MCT) using stratified randomization by sex using the Excel software RANDBETWEEN function (Microsoft) by S.C.F. Half of each group was female (50%). Group sizes (MCT, n = 6; SEFA-6179, n = 8) were predetermined for a target final sample size of 5 or 6 piglets per group, based on a power of 0.80 to detect a 2–standard deviation difference with an alpha of 0.05 on a 2-sample *t* test. Recent work using a neonatal piglet model with soybean oil lipid emulsion had a total bilirubin of approximately 1.7 ± 0.4 mg/dL (mean ± standard deviation based on n = 8), which would allow a significant difference of 0.8 mg/dL in total bilirubin to be determined.[16]

Intervention—Medium-Chain Triglyceride Vehicle Control or Study Drug

Piglets were treated daily by orogastric gavage using a temporarily placed 8 Fr nasogastric feeding tube with Dobhoff tip (Cardinal Health). The control group received isovolumetric (3 mL/kg/d) MCT vehicle. The treatment group received SEFA-6179 at 48 mg/kg/d dissolved in MCT vehicle.

Routine Medications

Whole sow blood was collected in citrate phosphate double dextrose solution (Haemonetics), sterilely aliquoted in a class II biosafety cabinet into 50-mL conical tubes and centrifuged to obtain plasma at 1200*g* × 60 minutes at 20°C. Maternal plasma was provided intravenously over the first 24 hours of life for passive immunity (5 mL/kg every 8 hours for 3 doses). Cefazolin (20 mg/kg) was provided twice daily for central line–associated bloodstream infection prophylaxis. No additional antibiotics were necessary. Daily intravenous famotidine (1 mg/kg) was administered for gastric acid hypersecretion prophylaxis.

Animal Care, Monitoring, and Humane Endpoints

Piglets were cohoused with 2 piglets per incubator with a 12-hour light/dark cycle and monitored for 24 hours per day. To minimize confounding, piglets were numbered and housed according to birth order regardless of treatment group, and order of treatment was alternated daily. Piglets were assessed daily for weight, temperature, activity, hydration, diarrhea, and skin breakdown. Additional blood chemistries were obtained for suspected hypovolemia or lethargy. At the discretion of the large-animal veterinarian, supplemental fluids (eg, normal saline or sodium bicarbonate 150 mEq/L) were provided for hypovolemia or acidosis. Early euthanasia was at the discretion of the large animal veterinarian (A.P.N.) for refractory signs of distress including fever (>40°C), hypoxia, respiratory distress, persistent lethargy, or immobility. Veterinary staff were blinded to group allocation.

Blood Collection and Biochemical Assessment

Blood was collected via central venous catheters on DOL 1 (before initiation of TPN), DOL 8, and DOL 15 (immediately before sacrifice) into lithium heparin plasma separator tubes (BD Microtainer). Plasma was obtained by centrifugation at 2000*g* × 15 minutes at 20°C. Plasma total bilirubin and direct bilirubin were performed by the Boston Children's Hospital clinical laboratory. Other biochemical markers were assessed using the VetScan VS2 (Zoetis). Serum adiponectin was assessed using a commercially available enzyme-linked

immunosorbent assay according to manufacturer's instructions (Biomatik EKN43266, Kitchener).

Sacrifice and Tissue Collection

Piglets were sacrificed on DOL 15 with sodium pentobarbital (110 mg/kg). Formalin-fixed, paraffin-embedded liver tissue was stained for H&E and Masson's trichrome. Frozen liver tissue embedded in optimal cutting temperature compound (Tissue-Tek) was stained with Oil Red O. Formalin-fixed, paraffin-embedded liver sections were stained using 3,3′-diaminobenzidine tetra hydrochloride immunohistochemistry (see Supplementary Material) by HistoWiz Inc. for α smooth muscle actin (αSMA) (Abcam ab5694) and cytokeratin 7 (Abcam ab181598). Quantification of tissue staining (Oil Red O: 10 randomly selected 200× fields; αSMA/cytokeratin 7: 5 randomly selected 0.2 × 0.2–cm fields) was performed using ImageJ (version 1.53a, National Institutes of Health) and the IHCToolbox plugin.[18,19] Tissue triglyceride content of liver tissue flash frozen in liquid nitrogen was quantified using a commercially available triglyceride assay according to the manufacturer's instructions (Abcam ab65336). Liver fibrosis was assessed on Masson's trichrome–stained slides by a masked veterinary pathologist using the Ishak fibrosis score.

Messenger RNA Sequencing and Transcriptomic Analysis

Liver tissue was collected at necropsy, flash frozen in liquid nitrogen, and stored at −80°C until analysis. Messenger RNA sequencing (RNA-Seq) was performed by Novogene Co. Differentially expressed genes were determined using the DESeq2 R package 1.20.0.[20] Adjusted P values of $< .05$ using the Benjamini-Hochberg approach for multiple testing were used for Gene Ontology (GO) and Kyoto Encyclopedia of Genes and Genomes (KEGG) enrichment analysis using clusterProfiler.[21] Further functional pathway analysis and investigation of upstream regulators was performed using Ingenuity Pathway Analysis (IPA) (Qiagen Inc.) using differentially expressed genes with an adjusted P of $< .1$ and log2 fold change of $>|0.5|$.[22] RNA-Seq data are filed in the National Center for Biotechnology Information Gene Expression Omnibus.[23] Detailed methods are provided in the Supplementary Material.

G Protein–Coupled Receptor 84, Peroxisome Proliferator-Activated Receptor α, and Peroxisome Proliferator-Activated Receptor γ Activation Assays

The activity of SEFA-6179 toward GPR84 was determined in vitro using a Hit Hunter 3′-5′-cyclic adenosine monophosphate (cAMP) assay (Eurofins DiscoverX) with embelin acting as a positive control. The activity of SEFA-6179 toward human PPARα and PPARγ was determined in vitro using PathHunter nuclear hormone receptor cell lines (Eurofins DiscoverX) with GW7647 or troglitazone acting as respective positive controls. Full methodology is provided in the Supplementary Material.

Preliminary Cohort

A preliminary cohort was used to establish the preterm piglet model. Piglets were delivered 4 days preterm and provided 14 days of TPN, resulting in cholestasis and liver fibrosis in control piglets receiving MCT vehicle treatment. Piglets receiving SEFA-6179 (24 mg/kg/d) did not develop cholestasis. Two of 4 MCT piglets (50%) and 5 of 7 SEFA-6179 piglets (71%) survived to DOL 15. Modifications to the study design were made to prevent infectious complications (daily cefazolin instead of cycled , 4-day on/4-day off cefazolin) and acute renal failure (increased TPN volume) encountered in this cohort (Supplementary Figure 1 and Supplementary Table 1).

Statistical Analysis

The distribution of each outcome was assessed by Shapiro-Wilk test. Continuous outcomes were assessed using nonparametric methods because the central limit theorem could not be relied on because of the small sample size. Because of the sample size, the analysis was not stratified by sex. At prespecified timepoints, comparison between 2 groups was performed with the exact Wilcoxon rank sum test. Animals with early euthanasia were excluded from the analysis because mortality occurred before the DOL 8 timepoint; all other data were included. Mean change in continuous outcomes, adjusted for baseline values, was reported from analysis of covariance (ANCOVA) with P values from rank-based ANCOVA. To determine the robustness of the results, parametric tests were also used (t test and ANCOVA, as appropriate), and in all cases the interpretation of the result was consistent for both tests. Assessment of TPN volume delivered was performed via area under the curve (AUC), calculated using the trapezoidal method as $AUC = 0.5 \times \Sigma\,[(T_{i+1} - T_i) * (Y_{i+1} + Y_i)]$. When divided by the number of observation days, this can be interpreted as a weighted average of the outcome. Group comparisons of the weighted average of the outcome were made by the exact Wilcoxon rank sum test. Assessment of the categorical outcome of Ishak fibrosis score was performed using the Fisher exact test. All tests of significance are 2 sided, with $P < .05$ considered statistically significant. Continuous outcomes are reported as median (range). Statistical analysis was conducted in SAS (version 9.4) by P.D.M.

Transcript Profiling

RNA-Seq data are available from the National Center for Biotechnology Information Gene Expression Omnibus, accession GSE223347.

Results

SEFA-6179 Activates G Protein–Coupled Receptor 84, Peroxisome Proliferator-Activated Receptor α, and Peroxisome Proliferator-Activated Receptor γ In Vitro

The chemical structure of SEFA-6179 is shown in comparison to decanoic acid, a 10-carbon MCFA (Figure 2*A* and *B*). The activity of SEFA-6179 toward GPR84, PPARγ, and PPARα was assessed in vitro compared to full agonists embelin, GW7647, and troglitazone, respectively (Figure 2*C*–*H*). Based on these assays, SEFA-6179 is a partial GPR84 agonist (69% efficacy, half maximal effective concentration [EC_{50}] = 12 μmol/L), a partial PPARα agonist (59% efficacy, EC_{50} = 4.4

HEPATOBILIARY

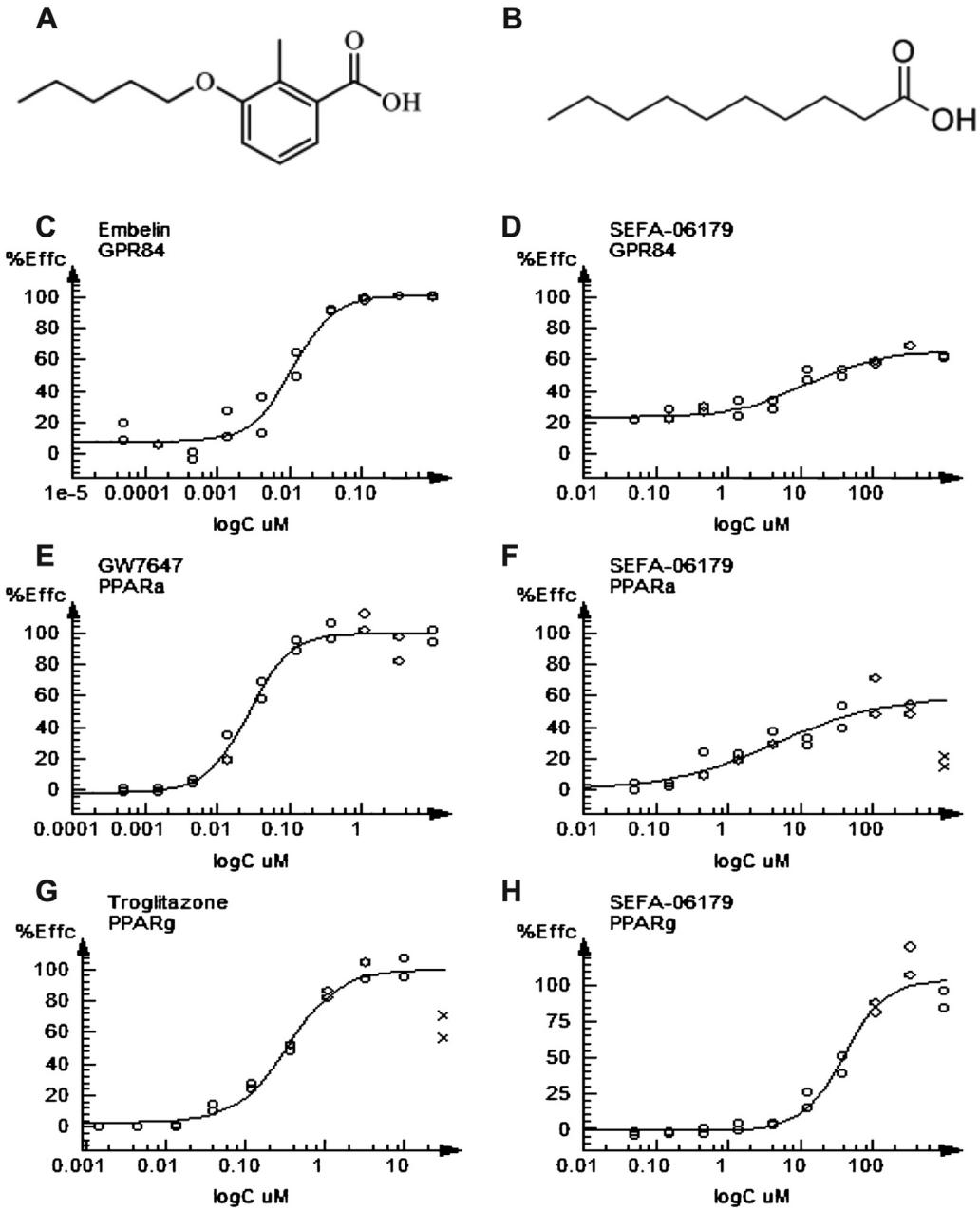

Figure 2. In vitro, SEFA-6179 is a GPR84 partial agonist, PPARα partial agonist, and PPARγ full agonist. The chemical structure of (*A*) SEFA-6179 is shown in comparison to (*B*) decanoic acid. (*C*, *D*) GPR84 activity of SEFA-6179 was determined using a Hit Hunter (Eurofins DiscoverX) 3′-5′-cyclic adenosine monophosphate (cAMP) assay with embelin acting as a positive control. (*E*, *F*) PPARα activity of SEFA-6179 was determined using PathHunter (Eurofins DiscoverX) nuclear hormone receptor cell lines with GW7647 as a positive control. (*G*, *H*) PPARγ activity of SEFA-6179 was determined using PathHunter nuclear hormone receptor cell lines with troglitazone as a positive control. Effc, efficacy; uM, μmol/L.

μmol/L), and a full PPARγ agonist (100% efficacy, $EC_{50} = 40$ μmol/L).

Preterm Piglets Treated With Medium-Chain Triglycerides or SEFA-6179 Received Similar Parenteral Nutrition and Gained Similar Weight

A preliminary cohort of piglets was used to establish the model (Supplementary Figure 1 and Supplementary Table 1). Yorkshire piglets were delivered 5 days preterm (111-day gestation). After resuscitation, all piglets had central venous catheters inserted on DOL 1, and TPN was initiated. Piglets were randomized to isovolumetric MCT vehicle control (3 mL/kg/d) or SEFA-6179 treatment (48 mg/kg/d).

Nutritional outcomes are shown in Figure 3. Piglets in each group received similar TPN volume (Figure 3*A*). Piglets in the MCT and SEFA-6179 groups gained similar weight

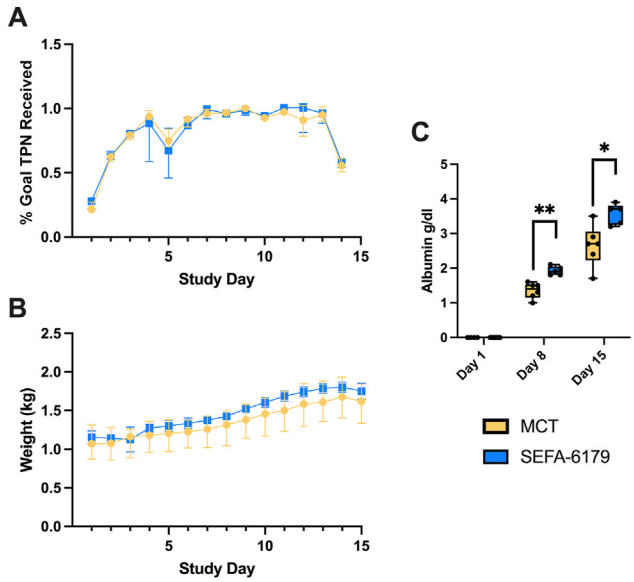

Figure 3. Nutritional outcomes in preterm piglets receiving 14 days of TPN. Piglets receiving MCT vehicle received (*A*) similar TPN volume and (*B*) gained similar weight as piglets receiving SEFA-6179 (median with interquartile range). (*C*) Compared to MCT, piglets receiving SEFA-6179 had higher plasma albumin on days of life 8 and 15 (boxplot with range). Comparison of weight gain was assessed using rank-based ANCOVA, and comparison of TPN volume was assessed by mean area under the curve and exact Wilcoxon rank sum. Comparisons of plasma albumin were done with exact Wilcoxon rank sum tests. *$P < .05$, **$P < .01$.

(0.44 [0.31–0.55] vs 0.59 [0.52–0.68] kg, $P = .15$) (Figure 3*B*). In both groups, plasma albumin increased from largely undetectable at birth through DOL 15. Compared to the MCT group, SEFA-6179 piglets had higher plasma albumin at DOL 8 and 15 (DOL 8: 1.5 [<1–1.6] vs 1.9 [1.8–2.1] g/dL, $P = .004$; DOL 15: 2.7 [1.7–3.5] vs 3.7 [3.2–3.9] g/dL, $P = .02$) (Figure 3*C*). Six of 6 (100%) MCT piglets and 5 of 8 (63%) SEFA-6179 piglets survived to DOL 15. The primary cause of mortality was renal failure. Necropsy findings are shown in Supplementary Table 2.

SEFA-6179 Prevented Biochemical Cholestasis at Day of Life 15

The primary study outcome was biochemical cholestasis. Biochemical markers of cholestasis are shown in Figure 4. Piglets in the MCT group developed a direct hyperbilirubinemia consistent with biochemical cholestasis at DOL 15, while the direct bilirubin remained normal in SEFA-6179 piglets (1.9 [0.3–2.8] vs <0.2 [<0.2–0.5] mg/dL, $P = .01$). Similarly, total bilirubin at DOL 15 was markedly elevated in the MCT group compared to the SEFA-6179 group (2.7 [0.8–4.9] vs 0.4 [0.4–1.3] mg/dL, $P = .02$). Plasma bile acids were elevated in MCT piglets at DOL 15 compared to SEFA-6179 (15 [<1–38] vs <1 [<1–8] μmol/L, $P = .03$). Gamma glutamyl transferase, a marker of cholangiocyte injury,[24] was also elevated at DOL 15 in the MCT piglets compared to SEFA-6179 piglets (172 [36–370] vs 30 [29–44] U/L, $P = .01$).

SEFA-6179 Prevented Liver Steatosis, Prevented Bile Duct Proliferation, and Reduced the Ishak Fibrosis Stage

Secondary outcomes included histologic biomarkers of progressive and/or chronic IFALD. Representative histology is shown in Figure 5. MCT piglets demonstrated steatosis, bile duct proliferation, and bridging portal-portal and portal-central vein fibrosis. SEFA-6179 piglets demonstrated minimal steatosis, only mild bile duct proliferation, and minimal fibrotic portal expansion. Steatosis was quantified first by staining frozen liver sections with Oil Red O; MCT piglets demonstrated increased Oil Red O staining compared to SEFA-6179 piglets (4.8% [1.0%–9.3%] vs 0.3% [0.0%–2.6%] area stained, $P = .02$) (Figures 5*C* and *D* and 6*A*). Liver tissue triglyceride content was also substantially higher in the MCT piglets compared to SEFA-6179 piglets (45.6 [20.4–55.9] vs 13.9 [12.8–21.1] mg triglycerides/g liver tissue, $P = .009$) (Figure 6*B*). Bile duct proliferation was assessed using immunohistochemical staining for cytokeratin 7, a cholangiocyte marker. MCT piglets demonstrated increased cytokeratin 7 staining compared to SEFA-6179 piglets, consistent with increased bile duct proliferation (1.6% [1.1%–2.1%] vs 0.5% [0.4%–1.1%] area stained, $P = .009$) (Figures 5*E* and *F* and 6*C*).

Hepatic stellate cell activation—a key step in fibrogenesis—was assessed using immunohistochemical staining for αSMA. MCT piglets demonstrated increased αSMA staining compared to SEFA-6179 piglets, consistent with increased hepatic stellate cell activation (3.0% [2.8%–5.2%] vs 1.8% [1.6%–2.8%] area stained, $P = .004$) (Figures 5*G* and *H* and 6*D*). A masked veterinary pathologist assessed liver fibrosis on formalin-fixed, paraffin-embedded liver tissue stained with Masson's trichrome (Figures 5*I* and *J* and 6*E*). MCT piglets had more severe fibrosis than SEFA-6179 piglets with a median Ishak fibrosis score of 3 (fibrous expansion of most portal areas with occasional portal-portal bridging) vs a median score of 1 (fibrous expansion of some portal areas ± short fibrous septa) ($P = .007$).

Key Functional Pathways Activated by SEFA-6179 Include Increased Fatty Acid β-Oxidation and Retinol/Retinoid X Receptor–Mediated Signaling, and Inflammatory Pathways Are Inhibited

We next focused on differences in gene expression between the 2 groups to identify key pathways mediating the hepatoprotective effects of SEFA-6179 demonstrated in this model. In vitro, SEFA-6179 is a GPR84/PPARα/PPARγ agonist, a receptor profile that would be expected to have broad inhibitory and stimulatory effects on inflammatory and metabolic pathways, respectively. Serum adiponectin, a sensitive and specific marker of PPARγ activation,[25] was elevated in the SEFA-6179 piglets at DOL 15 compared to

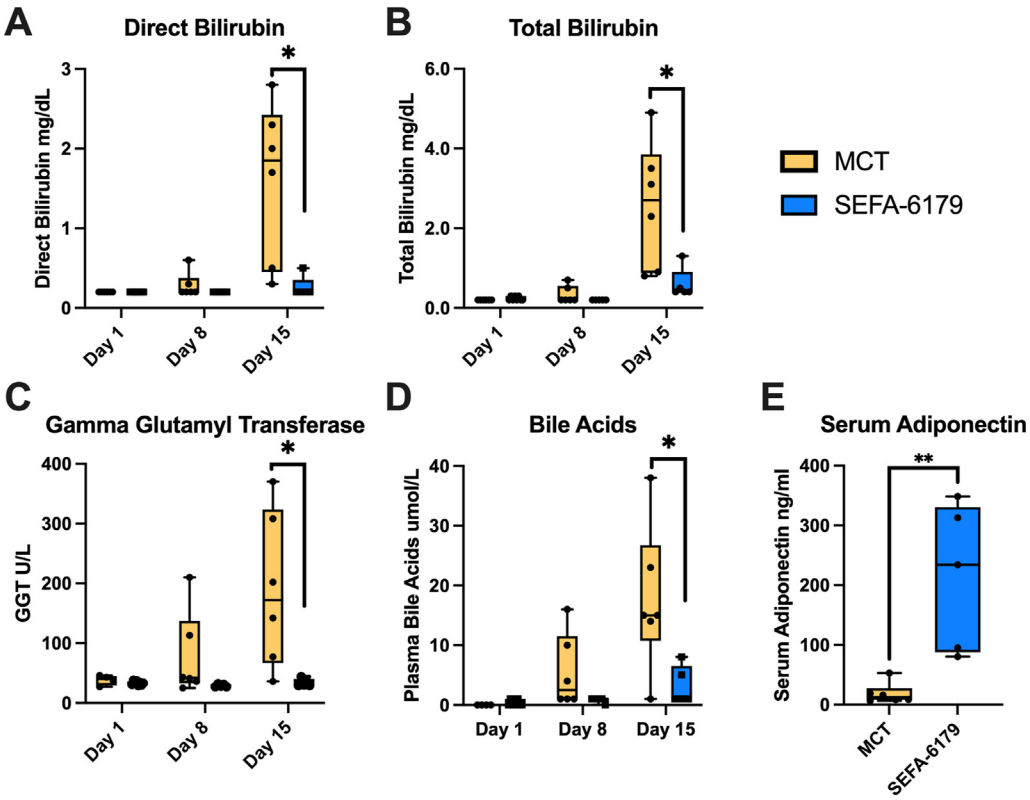

Figure 4. SEFA-6179 prevents biochemical cholestasis and increases serum adiponectin. Piglets received daily orogastric gavage of MCT vehicle or SEFA-6179. Serum adiponectin was assessed at DOL 15. Boxplots with range. Comparisons between MCT and SEFA-6179 piglets at DOL 1, 8, and 15 were performed with exact Wilcoxon rank sum tests. $^{*}P < .05$, $^{**}P < .01$.

the MCT piglets (234.1 [80.5–348.6] vs 12.5 [6.5–53.1] ng/mL, $P = .004$) (Figure 4*E*).

Messenger RNA-Seq was performed on liver tissue from all MCT and SEFA-6179 piglets. A total of 147 differentially expressed genes (52 up, 95 down) were identified (Figure 7*A*). Functional analysis was performed using GO, KEGG, and IPA (Figure 7*B–D*). Commonly enriched pathways across multiple functional analyses included fatty acid oxidation and metabolic processes (GO, KEGG, and IPA), retinol metabolism/retinoid X receptor (RXR) function (KEGG and IPA), and inflammation/cellular adhesion (GO and IPA).

GO enrichment analysis demonstrated that the most enriched biological processes were fatty acid oxidation and lipid oxidation, and the most enriched cellular components were involved in cell adhesion (Figure 7*B*). KEGG analysis found that the most enriched pathways involved retinol metabolism, PPAR signaling, and fatty acid degradation (Figure 7*C*). IPA demonstrated that the key up-regulated canonical pathways from SEFA-6179 treatment included pathways involved in oxidative phosphorylation, eukaryotic initiation factor 2 signaling, fatty acid β-oxidation I, and glutathione redox reactions I (Figure 7*D*). Both eukaryotic initiation factor 2 phosphorylation and glutathione redox reactions are critical in mediating the antioxidant capacity in the liver and responding to oxidative stress.[26] Key down-regulated canonical pathways from SEFA-6179 treatment included the sirtuin signaling pathway, granzyme A signaling, and lipopolysaccharide (LPS)/interleukin (IL) 1–mediated inhibition of RXR function.

Specific canonical pathways of interest were also analyzed in IPA based on observed differentially expressed genes. In the SEFA-6179–treated piglets, PPARα/RXR activation was predicted with increased fatty acid oxidation, fatty acid uptake, glucose homeostasis, lipoprotein metabolism, β-oxidation, and anti-inflammation (Supplementary Figure 2). Consistent with this activation, investigation of the inhibited LPS/IL1–mediated inhibition of RXR function pathway (Supplementary Figure 3) demonstrates predicted activation of RXR-mediated pathways including master regulators liver X receptor, farsenoid X receptor, retinoic acid receptor, pregnane X receptor, and PPARs. Notably, this includes genes involved in bile acid and organic ion transport in addition to fatty acid metabolism. Nuclear factor κB (NF-κB) signaling (which is down-regulated by both PPARγ and PPARα agonism) was predicted to be inhibited (Supplementary Figure 4). Finally, hepatic fibrosis signaling was investigated (Supplementary Figure 5). Fibrosis pathways mediated by transforming growth factor β (TGF-β), suppressor of mothers against decapentaplegic (SMAD) 2/3/4, c-Jun N-terminal kinase (JNK), and signal transducer and activator of transcription 3 (STAT3) were predicted to be inhibited with downstream decreased hepatic stellate cell activation and liver fibrosis.

Predicted Upstream Regulators of Differentially Expressed Genes/Pathways Are Consistent With G Protein–Coupled Receptor 84, Peroxisome Proliferator-Activated Receptor α, and Peroxisome Proliferator-Activated Receptor γ Agonism

Upstream regulator analysis by IPA identified candidate upstream regulators consistent with observed downstream pathway enrichment from SEFA-6179 treatment (Supplementary Table 3). The activation *z*-score provides the degree of downstream activation or inhibition, with upstream regulators with a *z*-score of $>|2|$ considered significant. Identification of PPARγ coactivator 1α (PPARGC1A) as one of the greatest activated upstream regulators (*z*-score of 3.234) is consistent with PPARγ agonism (because it is a transcriptional coactivator for PPARγ). Similarly, hepatocyte nuclear factor 4 alpha (HNF4A) interacts with PPARα to drive fatty acid metabolism, consistent with activation of pathways downstream of PPARα. Inhibited upstream regulators included proinflammatory signaling molecules, such as myeloid differentiation primary response 88 and tumor necrosis factor—consistent with anti-inflammatory effects. Multiple transcription regulators were identified as possible activated upstream regulators that all inhibit transcription of collagen genes *COL1A2* and *COL3A1*, consistent with downstream antifibrotic activity. Eukaryotic initiation factor 6 inhibition is also associated with reduction in nonalcoholic fatty liver disease through down-regulation of de novo lipogenesis genes and collagen-encoding genes, resulting in decreased steatosis and fibrosis.[27] Predicted upstream regulators are consistent with GPR80, PPARα, and PPARγ agonism as the key mechanisms mediating the metabolic, anti-inflammatory, and antifibrotic effects of SEFA-6179 in this model.

Discussion

Here, we demonstrate that SEFA-6179 prevents IFALD in a cholestatic preterm piglet model. The swine gastrointestinal system is highly similar to that of humans with respect to intestinal and biliary physiology, intestinal absorption, hormonal regulation, and nutritional requirements.[28] The neonatal piglet model of IFALD closely reproduces the pathophysiology of human IFALD. Administration of TPN to neonatal piglets—especially with preterm delivery, a key risk factor in human IFALD—results in cholestatic liver disease with both biochemical and histologic biomarkers that parallel human disease.[15,16,29,30] In this study, piglets receiving MCT vehicle developed active cholestatic disease, marked by elevated plasma biomarkers (direct bilirubin, total bilirubin, gamma glutamyl transferase, bile acids) and histologic liver injury with early progression to steatosis, bile duct proliferation, and fibrosis. SEFA-6179 prevented cholestasis and steatosis and reduced bile duct proliferation and fibrosis. Transcriptome analysis demonstrated that SEFA-6179 activated anti-inflammatory pathways, fatty acid β-oxidation, and antifibrotic pathways consistent with GPR84, PPARα, and PPARγ activation.

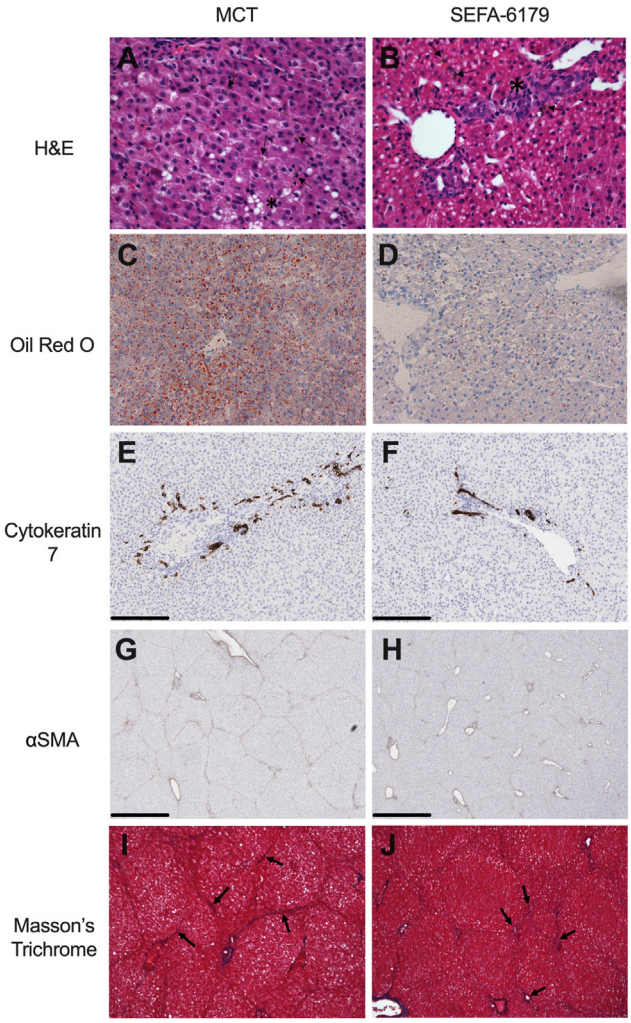

Figure 5. MCT piglets show steatosis, bile duct proliferation, and fibrosis on representative liver histology, which is reduced by SEFA-6179 treatment. (*A*, *B*) Formalin-fixed, paraffin-embedded liver sections were stained with H&E. (*C*, *D*) Frozen liver sections were stained with Oil Red O. (*E–H*) Immunohistochemical staining (3,3′-diaminobenzidine tetra hydrochloride, *brown*) of formalin-fixed, paraffin-embedded liver sections was performed for (*E*, *F*) cytokeratin 7 and (*G*, *H*) αSMA. (*I*, *J*) Formalin-fixed, paraffin-embedded liver sections were stained with Masson's trichrome. MCT piglets demonstrate steatosis (*A*, *asterisks* and *C*), extensive bile pigment (*A*, *arrows*), bile duct proliferation (*E*), extensive αSMA staining (*G*), and fibrosis indicated by bridging portal-portal and portal-central vein fibrosis (*I*, *arrows*). SEFA-6179 piglets demonstrate no steatosis (*D*), mild bile pigment (*B*, *arrows*), mild bile duct proliferation (*B*, *asterisks* and *F*), reduced αSMA staining (*H*), and minimal fibrotic portal expansion (*J*, *arrows*). Original magnifications: (*A*) 400×, (*B*) 200×, (*C*) 200-nm reference bars, (*D*) 1-mm reference bars, and (*E*) 100×.

Advances in modern management of intestinal failure have allowed patients to survive years or even decades on parenteral nutrition. Fish oil lipid emulsion and hepatoprotective management have transformed IFALD into a chronic liver disease, but few therapeutic options exist to interrupt further disease progression. Current estimates suggest that 20%–30% of children with intestinal failure

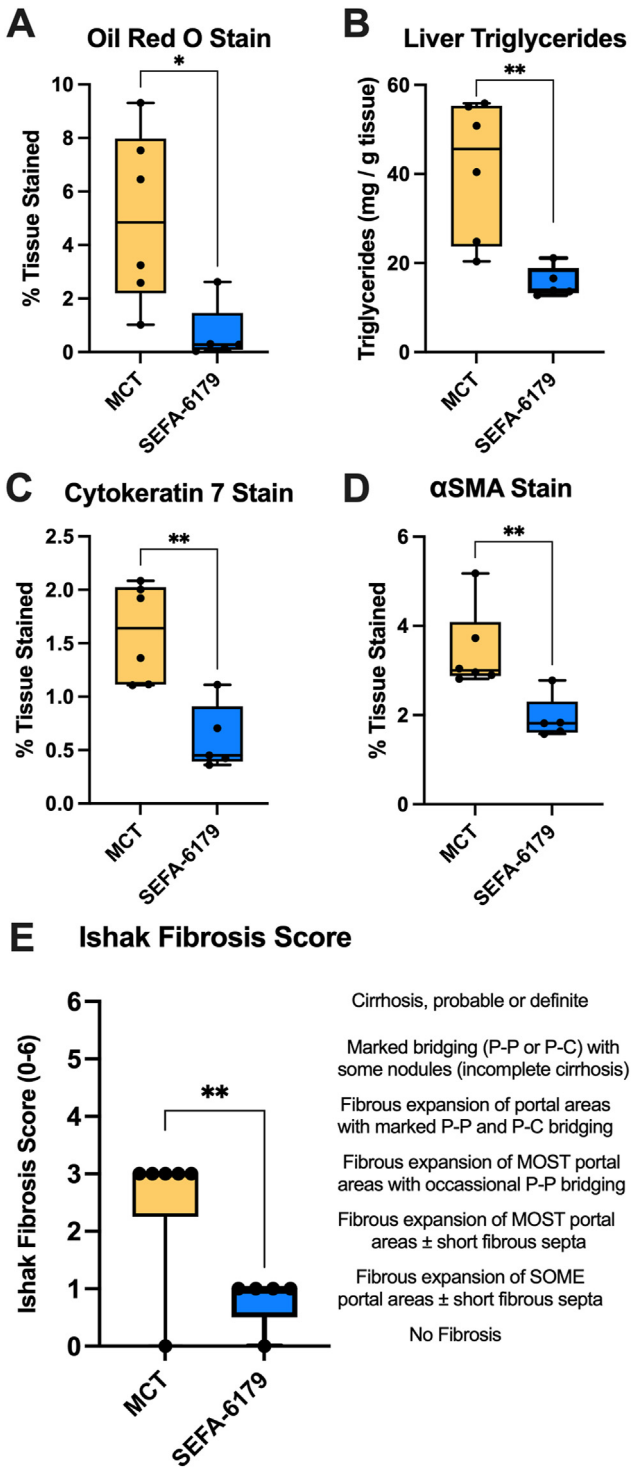

Figure 6. SEFA-6179 reduces liver steatosis, bile duct proliferation, hepatic stellate cell activation, and Ishak fibrosis score. SEFA-6179 piglets, compared to MCT piglets, demonstrated decreased (*A*) Oil Red O staining and (*B*) liver triglyceride content consistent with minimal hepatosteatosis, (*C*) decreased cytokeratin 7 staining consistent with minimal bile duct proliferation, (*D*) decreased αSMA staining consistent with decreased hepatic stellate cell activation, and (*E*) decreased Ishak fibrosis score assessed by a masked pathologist. Boxplots with range. Comparisons in *A–D* were made with exact Wilcoxon rank sum tests. The mean Ishak score is presented as a diamond. Ishak fibrosis scores were compared with the Fisher exact test. $^{*}P < .05$, $^{**}P < .01$. C, central; P, portal.

will develop overt IFALD, although this may be an underestimate of the true disease burden.[2] Recent literature has identified a new, poorly understood entity of noncholestatic IFALD marked by subclinical histologic progression with long-term parenteral nutrition, despite an absence of overt biochemical cholestasis. A recently published cohort from our center found that 79% of pediatric intestinal failure patients dependent on long-term parenteral nutrition have (typically mild to moderate) elevations in alanine aminotransferase.[8] IFALD is classified histologically into the active (cholestasis and inflammation) or chronic (steatosis and fibrosis) stage.[2] On routine liver biopsy of a modern cohort of pediatric patients with intestinal failure, two thirds demonstrated histologic liver disease: 48% had active IFALD, and 21% had chronic IFALD.[7] On subsequent biopsy of patients with active IFALD (median time between biopsies was 2.5 years), two thirds demonstrated either persistent active IFALD or transition to chronic IFALD. Even after weaning from parenteral nutrition, most pediatric patients with intestinal failure will have persistent fibrosis, and half will have steatosis on biopsy.[31] A major need exists for therapeutics to both prevent the development of IFALD and interrupt the progression of established disease. Our results suggest that SEFA-6179 may prevent development of IFALD; further research is necessary to investigate whether SEFA-6179 can interrupt the progression of established disease.

IFALD in premature neonates is characterized by an inflammatory and cholestatic phenotype. The immature liver is poorly able to handle the numerous inflammatory insults in this population, including proinflammatory lipids and phytosterols, translocation of bacterial products across a disrupted intestinal epithelium into the portal circulation, and sepsis from necrotizing enterocolitis or central line–associated bloodstream infections.[2] Even with newer-generation mixed oil lipid emulsions with a decreased (more anti-inflammatory) $\omega 6{:}\omega 3$ fatty acid ratio and reduced phytosterols, IFALD still occurs at a high incidence in susceptible patient populations.[32] GPR84 activation has recently been identified as a hepatoprotective MCFA receptor, exhibiting both anti-inflammatory and antifibrotic activity in response to lipotoxicity via down-regulation of macrophage activation.[12] Although MCFAs are established endogenous ligands, GPR84 remains an orphan receptor because its downstream signaling has not been fully elucidated.[14] Importantly, SEFA-6179 has a similar potency toward GPR84 as naturally occurring MCFAs (low micromolar range), a potential differentiating factor from highly potent synthetic GPR84 agonists that display proinflammatory effects.[12]

A key proposed mechanism of IFALD is an inflammatory response to bacterial products, either from recurrent sepsis (eg, from central line–associated bloodstream infection) or from absorption into the portal circulation.[2] Several lines of evidence support the role of enteric bacterial products in development of IFALD: patients with short bowel syndrome have increased intestinal permeability, small bowel bacterial overgrowth/dysbiosis is associated with Gram-negative bloodstream infections and IFALD progression, and

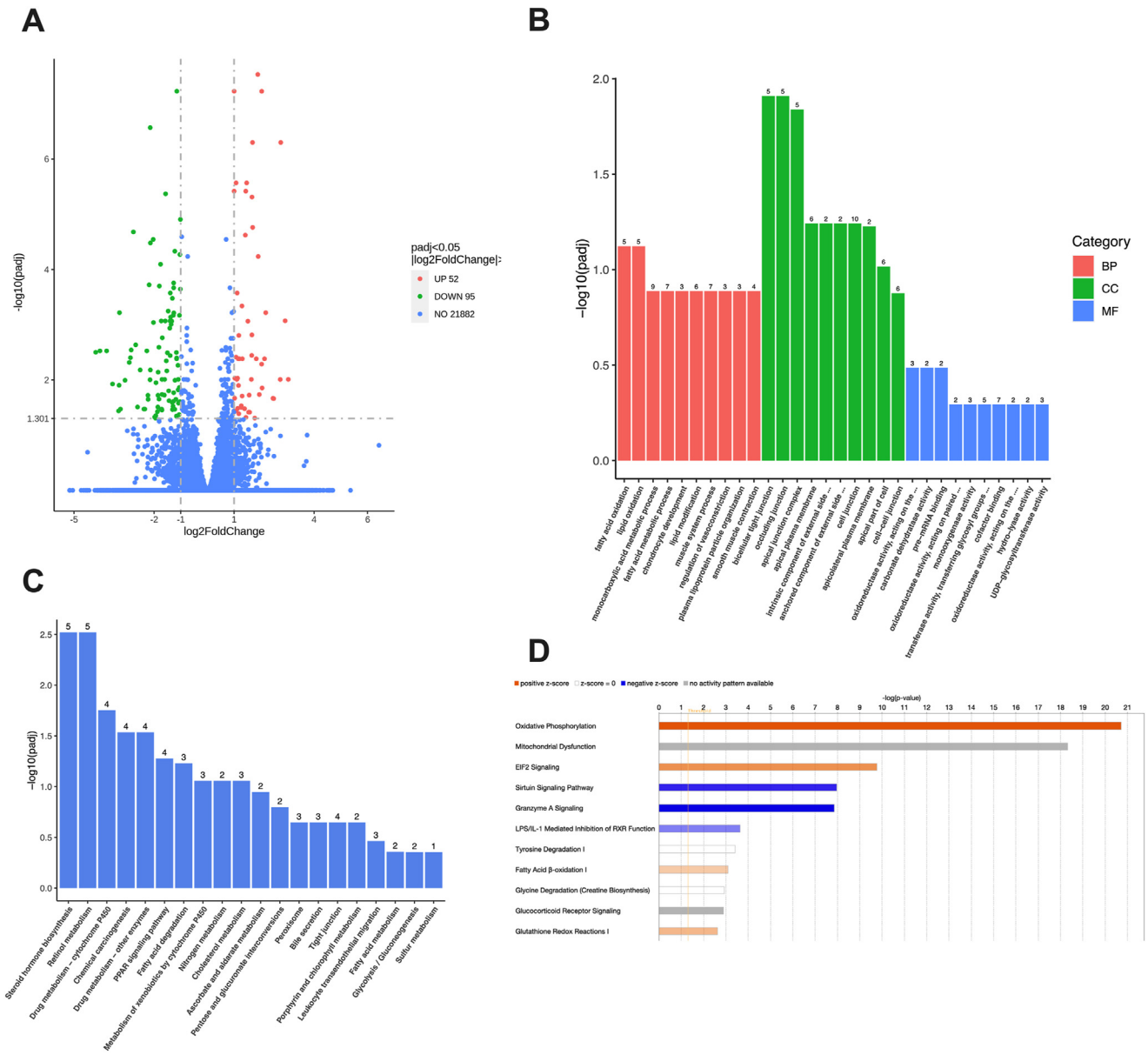

Figure 7. RNA-Seq demonstrates enrichment of fatty acid oxidation, retinal metabolism, and PPAR signaling from SEFA-6179 treatment. (*A*) RNA-Seq was performed on the Illumina NovaSeq 6000 platform, and differentially expressed genes were identified. (*B*) GO analysis demonstrated biological process (BP), cellular component (CC), and molecular function (MF) categories of commonly enriched genes, including fatty acid oxidation, lipid oxidation, and cellular adhesion. (*C*) KEGG analysis demonstrated key enriched pathways including retinol metabolism and PPAR signaling. (*D*) Key canonical pathways determined using IPA include increased oxidative phosphorylation and fatty acid β-oxidation, with down-regulated granzyme A signaling and LPS/IL1–mediated inhibition of RXR function.

flagellin and LPS (along with increased anti-flagellin/anti-LPS immunoglobulins) have been directly detected in serum samples from patients with short bowel syndrome.[33,34] Both PPARα and PPARγ have anti-inflammatory effects mediated by a variety of mechanisms that may interrupt the inflammatory liver response to bacterial products. Liver-specific PPARα agonism prevents the systemic inflammatory response induced by LPS–toll-like receptor 4 (TLR4) signaling.[35] In TLR4=knockout mouse models of IFALD and nonalcoholic steatohepatitis, TLR4$^{-/-}$ mice are protected from liver disease.[36,37] PPARα agonism also suppresses the IL6-induced acute phase response via down-regulation of interleukin 6 receptor components gp80 and gp130 (reducing downstream STAT3 and JNK signal transduction) and decreases expression of CCAAT enhancer-binding proteins (transcription factors for acute phase response genes).[38] Both PPARα and PPARγ inhibit the NF-κB pathway.[39,40] Furthermore, macrophage polarization to a M2 anti-inflammatory phenotype is driven by PPARγ.[41] On transcriptomic analysis of SEFA-6179 treatment, inhibition of the canonical pathways NF-κB and LPS/IL1 mediated inhibition of RXR function, as well as predicted inhibition of

transcription downstream from myeloid differentiation primary response 88 and tumor necrosis factor, was consistent with the anti-inflammatory effects of both PPARα and PPARγ agonism.

In adults with intestinal failure, IFALD is characterized by a steatosis-predominant phenotype. Minimizing parenteral lipids may drive de novo lipogenesis; alternatively, parenteral administration of lipids bypasses the normal physiologic trafficking of micelles with resultant first-pass metabolism occurring in the liver, which contributes to increased hepatic lipid deposition.[42] PPARα is a key ligand-activated transcription factor that regulates lipid transport and fatty acid oxidation in the liver, controlling the rate-limiting enzymes of peroxisomal β-oxidation and mitochondrial β-oxidation.[43] SEFA-6179 effectively prevented hepatosteatosis in this study. In nonalcoholic fatty liver disease, PPARα agonists, including clofibrate and fenofibrate, have little effect on biochemical and histologic disease, and multiple randomized controlled trials demonstrate that PPARγ agonists (rosiglitazone and pioglitazone) decrease liver enzymes, steatosis, and inflammation but minimally affect fibrosis.[44] These findings suggest that dual PPARα and PPARγ agonism, in addition to GPR84 activation, may play an additive and/or synergistic role in the observed anti-inflammatory, antisteatotic, and antifibrotic effects.

Multiple pathways may mediate the antifibrotic effects of SEFA-6179. Anti-inflammatory effects mediated by GPR84, PPARα, and PPARγ may interrupt macrophage and hepatic stellate cell activation, resulting in decreased extracellular matrix deposition. In addition to down-regulation of inflammation, PPARγ inhibits hepatic stellate cell activation through modulation of TGF-β signaling pathways.[45] Decreased αSMA staining in the SEFA-6179 piglets is consistent with prevention of hepatic stellate cell activation. PPARγ agonists are effective in reducing fibrosis in models of pulmonary fibrosis, renal fibrosis, liver fibrosis, cardiac fibrosis.[46–49] A recent phase 2b double-blind, randomized, placebo-controlled trial of the pan-PPAR agonist lanifibranor in nonalcoholic steatohepatitis found substantial resolution of nonalcoholic steatohepatitis and an improvement in fibrosis stage.[50]

There are several important limitations to this work. The model used recapitulates the disease of the preterm neonate with cholestatic IFALD, but it may not be broadly applicable to older children and adults, who less frequently demonstrate a cholestasis-predominant phenotype. In addition, although most long-term parenteral nutrition patients have short bowel syndrome (from either a congenital or acquired cause), the piglets retained the entirety of their bowel. For an enterally administered therapy, this may be an important limitation, and careful pharmacokinetic investigation will be critical in translation to human populations. Because of the tenuous clinical status of premature piglets, all piglets required TPN for survival, and a "normal" control without TPN was not possible. Finally, in this study, SEFA-6179 was evaluated as a preventative treatment, and further investigations of its efficacy in treating established IFALD are warranted.

Despite advances in IFALD management with hepatoprotective strategies, many patients with intestinal failure have progressive chronic liver disease and fibrosis. IFALD remains a key life-limiting complication of intestinal failure. In a preterm piglet model of IFALD that is highly analogous to the preterm neonate with cholestatic IFALD, SEFA-6179 prevented cholestasis and steatosis and reduced bile duct proliferation and fibrosis. Transcriptomic analysis revealed that these effects are consistent with the demonstrated in vitro GPR84/PPARα/PPARγ agonism, with increased fatty acid metabolism; inhibition of key inflammatory pathways (NF-κB, IL1/LPS); and inhibition of fibrosis via TGF-β, SMAD 2/3/4, and JNK pathways. Further investigation will be critical to evaluate the efficacy of SEFA-6179 in chronic noncholestatic IFALD. SEFA-6179 has recently completed a phase 1 clinical trial and will soon begin a phase 2 clinical trial for the treatment of IFALD. The unique mechanism of action of SEFA-6179 (GPR84/PPARα/PPARγ agonism) may also provide a new avenue of investigation for other cholestatic liver diseases with limited therapeutic options.

Supplementary Material

Note: To access the supplementary material accompanying this article, visit the online version of *Gastroenterology* at www.gastrojournal.org, and at https://doi.org/10.1053/j.gastro.2023.05.035.

References

1. Lauriti G, Zani A, Aufieri R, et al. Incidence, prevention, and treatment of parenteral nutrition-associated cholestasis and intestinal failure-associated liver disease in infants and children: a systematic review. JPEN J Parenter Enteral Nutr 2014;38:70–85.
2. Khalaf RT, Sokol RJ. New insights into intestinal failure-associated liver disease in children. Hepatology 2020;71:1486–1498.
3. Christensen RD, Henry E, Wiedmeier SE, et al. Identifying patients, on the first day of life, at high-risk of developing parenteral nutrition-associated liver disease. J Perinatol 2007;27:284–290.
4. Lee WS, Chew KS, Ng RT, et al. Intestinal failure-associated liver disease (IFALD): insights into pathogenesis and advances in management. Hepatol Int 2020;14:305–316.
5. Gura KM, Premkumar MH, Calkins KL, et al. Fish oil emulsion reduces liver injury and liver transplantation in children with intestinal failure-associated liver disease: a multicenter integrated study. J Pediatr 2021;230:46–54.e2.
6. Secor JD, Yu L, Tsikis S, et al. Current strategies for managing intestinal failure-associated liver disease. Expert Opin Drug Saf 2021;20:307–320.
7. Mutanen A, Lohi J, Merras-Salmio L, et al. Prediction, identification and progression of histopathological liver disease activity in children with intestinal failure. J Hepatol 2021;74:593–602.

8. Keefe G, Culbreath K, Knell J, et al. Long-term assessment of bilirubin and transaminase trends in pediatric intestinal failure patients during the era of hepatoprotective parenteral nutrition. J Pediatr Surg 2022; 57:122–126.
9. **Huysentruyt K, Belza C**, Wong-Sterling S, et al. Use of a combined transient elastography and biochemical strategy to determine liver fibrosis in pediatric intestinal failure. Clin Nutr 2023;42:136–142.
10. Greenberger NJ, Rodgers JB, Isselbacher KJ. Absorption of medium and long chain triglycerides: factors influencing their hydrolysis and transport. J Clin Invest 1966;45:217–227.
11. Fougerat A, Montagner A, Loiseau N, et al. Peroxisome proliferator-activated receptors and their novel ligands as candidates for the treatment of non-alcoholic fatty liver disease. Cells 2020;9(7):1638.
12. **Ohue-Kitano R, Nonaka H**, Nishida A, et al. Medium-chain fatty acids suppress lipotoxicity-induced hepatic fibrosis via the immunomodulating receptor GPR84. JCI Insight 2023;8(2):e165469.
13. Sanyal AJ, Chalasani N, Kowdley KV, et al. Pioglitazone, vitamin E, or placebo for nonalcoholic steatohepatitis. N Engl J Med 2010;362:1675–1685.
14. Luscombe VB, Lucy D, Bataille CJR, et al. 20 years an orphan: is GPR84 a plausible medium-chain fatty acid-sensing receptor? DNA Cell Biol 2020; 39:1926–1937.
15. Vlaardingerbroek H, Ng K, Stoll B, et al. New generation lipid emulsions prevent PNALD in chronic parenterally fed preterm pigs. J Lipid Res 2014;55:466–477.
16. Ng K, Stoll B, Chacko S, et al. Vitamin E in new-generation lipid emulsions protects against parenteral nutrition-associated liver disease in parenteral nutrition-fed preterm pigs. JPEN J Parenter Enteral Nutr 2016; 40:656–671.
17. National Research Council. Guide for the care and use of laboratory animals. 8th ed. Washington, DC: National Academies Press, 2011. Available at: http://www.nap.edu/catalog/12910. Accessed October 31, 2022.
18. Schneider CA, Rasband WS, Eliceiri KW. NIH Image to ImageJ: 25 years of image analysis. Nat Methods 2012; 9:671–675.
19. Shu J, Qiu G, Mohammad I. A semi-automatic image analysis tool for biomarker detection in immunohistochemistry analysis. In: 2013 Seventh International Conference on Image and Graphics. Conference Publishing Services, IEEE, Washington, DC; 2013:937–942.
20. Love MI, Huber W, Anders S. Moderated estimation of fold change and dispersion for RNA-seq data with DESeq2. Genome Biol 2014;15:550.
21. Yu G, Wang L-G, Han Y, et al. clusterProfiler: an R package for comparing biological themes among gene clusters. OMICS 2012;16:284–287.
22. Krämer A, Green J, Pollard J, et al. Causal analysis approaches in Ingenuity Pathway Analysis. Bioinformatics 2014;30:523–530.
23. Fligor SC, Tsikis ST, Puder M. Transcriptomic analysis of SEFA-6179 treatment in preterm piglets receiving parenteral nutrition [dataset]. National Center for Biotechnology Information Gene Expression Omnibus. Available at: https://www.ncbi.nlm.nih.gov/geo/query/acc.cgi?&acc=GSM6945905. Accessed February 16, 2023.
24. Onofrio FQ, Hirschfield GM. The pathophysiology of cholestasis and its relevance to clinical practice. Clin Liver Dis 2020;15:110–114.
25. Lakota K, Wei J, Carns M, et al. Levels of adiponectin, a marker for PPAR-gamma activity, correlate with skin fibrosis in systemic sclerosis: potential utility as biomarker? Arthritis Res Ther 2012;14:R102.
26. **Choi W-G, Han J, Kim J-H**, et al. eIF2α phosphorylation is required to prevent hepatocyte death and liver fibrosis in mice challenged with a high fructose diet. Nutr Metab (Lond) 2017;14:48.
27. **Scagliola A, Miluzio A**, Ventura G, et al. Targeting of eIF6-driven translation induces a metabolic rewiring that reduces NAFLD and the consequent evolution to hepatocellular carcinoma. Nat Commun 2021; 12:4878.
28. Gonzalez LM, Moeser AJ, Blikslager AT. Porcine models of digestive disease: the future of large animal translational research. Transl Res 2015;166:12–27.
29. Guthrie G, Stoll B, Chacko S, et al. Depletion and enrichment of phytosterols in soybean oil lipid emulsions directly associate with serum markers of cholestasis in preterm parenteral nutrition-fed pigs. JPEN J Parenter Enteral Nutr 2022;46:160–171.
30. Isaac DM, Alzaben AS, Mazurak VC, et al. Mixed lipid, fish oil, and soybean oil parenteral lipids impact cholestasis, hepatic phytosterol, and lipid composition. J Pediatr Gastroenterol Nutr 2019;68:861–867.
31. Mutanen A, Lohi J, Heikkilä P, et al. Persistent abnormal liver fibrosis after weaning off parenteral nutrition in pediatric intestinal failure. Hepatology 2013;58: 729–738.
32. **Yu LJ, Anez-Bustillos L**, Mitchell PD, et al. Incidence and development of cholestasis in surgical neonates receiving an intravenous mixed-oil lipid emulsion. JPEN J Parenter Enteral Nutr 2023;47:30–40.
33. Cole CR, Frem JC, Schmotzer B, et al. The rate of bloodstream infection is high in infants with short bowel syndrome: relationship with small bowel bacterial overgrowth, enteral feeding, and inflammatory and immune responses. J Pediatr 2010;156:941–947.e1.
34. Ziegler TR, Luo M, Estívariz CF, et al. Detectable serum flagellin and lipopolysaccharide and upregulated anti-flagellin and lipopolysaccharide immunoglobulins in human short bowel syndrome. Am J Physiol Regul Integr Comp Physiol 2008;294(2):R402–R410.
35. Mansouri RM, Baugé E, Staels B, Gervois P. Systemic and distal repercussions of liver-specific peroxisome proliferator-activated receptor-α control of the acute-phase response. Endocrinology 2008;149:3215–3223.
36. Barron LK, Bao JW, Aladegbami BG, et al. Toll-like receptor 4 is critical for the development of resection-associated hepatic steatosis. J Pediatr Surg 2017; 52:1014–1019.
37. Sutter AG, Palanisamy AP, Lench JH, et al. Dietary saturated fat promotes development of hepatic

HEPATOBILIARY

inflammation through toll-like receptor 4 in mice. J Cell Biochem 2016;117:1613–1621.
38. **Gervois P, Kleemann R**, Pilon A, et al. Global suppression of IL-6-induced acute phase response gene expression after chronic in vivo treatment with the peroxisome proliferator-activated receptor-α activator fenofibrate. J Biol Chem 2004;279:16154–16160.
39. Kleemann R, Gervois PP, Verschuren L, et al. Fibrates down-regulate IL-1-stimulated C-reactive protein gene expression in hepatocytes by reducing nuclear p50-NFκB-C/EBP-β complex formation. Blood 2003; 101:545–551.
40. Scirpo R, Fiorotto R, Villani A, et al. Stimulation of nuclear receptor peroxisome proliferator–activated receptor-γ limits NF-kB-dependent inflammation in mouse cystic fibrosis biliary epithelium. Hepatology 2015;62: 1551–1562.
41. Yao Q, Liu J, Zhang Z, et al. Peroxisome proliferator–activated receptor γ (PPARγ) induces the gene expression of integrin αVβ5 to promote macrophage M2 polarization. J Biol Chem 2018;293:16572–16582.
42. Guthrie G. Parenteral nutrition associated hepatic steatosis and NAFLD intersect at AMPK. Cell Mol Gastroenterol Hepatol 2022;14:724–725.
43. Pawlak M, Lefebvre P, Staels B. Molecular mechanism of PPARα action and its impact on lipid metabolism, inflammation and fibrosis in non-alcoholic fatty liver disease. J Hepatol 2015;62:720–733.
44. Liss KHH, Finck BN. PPARs and nonalcoholic fatty liver disease. Biochimie 2017;136:65–74.
45. Kon K, Ikejima K, Hirose M, et al. Pioglitazone prevents early-phase hepatic fibrogenesis caused by carbon tetrachloride. Biochem Biophys Res Commun 2002; 291:55–61.
46. Avouac J, Konstantinova I, Guignabert C, et al. Pan-PPAR agonist IVA337 is effective in experimental lung fibrosis and pulmonary hypertension. Ann Rheum Dis 2017;76:1931–1940.
47. Németh Á, Mózes MM, Calvier L, et al. The PPARγ agonist pioglitazone prevents TGF-β induced renal fibrosis by repressing EGR-1 and STAT3. BMC Nephrol 2019;20(1):245.
48. **Boyer-Diaz Z, Aristu-Zabalza P**, Andrés-Rozas M, et al. Pan-PPAR agonist lanifibranor improves portal hypertension and hepatic fibrosis in experimental advanced chronic liver disease. J Hepatol 2021; 74:1188–1199.
49. Ogata T, Miyauchi T, Sakai S, et al. Stimulation of peroxisome-proliferator-activated receptor α (PPAR α) attenuates cardiac fibrosis and endothelin-1 production in pressure-overloaded rat hearts. Clin Sci (Lond) 2002; 103(Suppl 48):284S–288S.
50. Francque SM, Bedossa P, Ratziu V, et al. A randomized, controlled trial of the pan-PPAR agonist lanifibranor in NASH. N Engl J Med 2021;385:1547–1558.

Author names in bold designate shared co-first authorship.

Received February 16, 2023. Accepted May 16, 2023.

Correspondence
Address correspondence to: Mark Puder, MD, PhD, Department of Surgery, Boston Children's Hospital, 300 Longwood Avenue, Fegan 3, Boston, Massachusetts 02115. e-mail: Mark.Puder@childrens.harvard.edu.

Acknowledgments
The authors would like to thank the certified veterinary technicians Robin Grammer and Brittany Pattison for their excellent care of the study animals.

CRediT Authorship Contributions
Scott C. Fligor, MD (Conceptualization: Equal; Funding acquisition: Supporting; Investigation: Lead; Methodology: Equal; Visualization: Lead; Writing – original draft: Lead; Writing – review & editing: Equal).

Savas T. Tsikis, MD (Investigation: Equal; Methodology: Equal; Writing – review & editing: Equal).

Thomas I. Hirsch, MD (Investigation: Equal; Writing – review & editing: Equal).

Amy Pan, BS (Investigation: Equal; Writing – review & editing: Supporting).

Kamila Moskowitzova, MD (Investigation: Supporting; Writing – review & editing: Equal).

Lorena Rincon-Cruz, MD (Investigation: Supporting; Writing – review & editing: Equal).

Ashlyn E. Whitlock, MD (Investigation: Supporting; Writing – review & editing: Equal).

Paul D. Mitchell, MS (Formal analysis: Lead; Methodology: Supporting; Visualization: Supporting; Writing – review & editing: Equal).

Arthur P. Nedder, DVM (Investigation: Supporting; Methodology: Equal; Writing – review & editing: Supporting).

Kathleen M. Gura, PharmD (Methodology: Supporting; Writing – review & editing: Equal).

David A. Fraser, PhD (Investigation: Supporting; Methodology: Supporting; Writing – review & editing: Supporting).

Mark Puder, MD, PhD (Conceptualization: Equal; Funding acquisition: Lead; Methodology: Equal; Supervision: Lead; Writing – review & editing: Equal).

Conflicts of interest
These authors disclose the following: This study was primarily funded via a sponsored research agreement with NorthSea Therapeutics. David A. Fraser is the chief scientific officer of NorthSea Therapeutics and was responsible for the in vitro analysis. Mark Puder and Kathleen M. Gura are external consultants for NorthSea Therapeutics. The study was designed in consultation with NorthSea Therapeutics, but final study design decisions were made by Mark Puder and Scott C. Fligor. Other than the in vitro analysis, NorthSea Therapeutics and David A. Fraser were not involved in the collection, analysis, or interpretation of data. The remaining authors disclose no conflicts.

Funding
This study was funded by NorthSea Therapeutics under a sponsored research agreement, National Institutes of Health grants 5T32HL007734 (to Scott C. Fligor and Thomas I. Hirsch) and 2T32DK007754-22 (to Savas T. Tsikis), the Beth Israel Deaconess Medical Center Richard and Sandra Cummings Research Fellowship (to Scott C. Fligor), the Boston Children's Hospital Vascular Biology Program, and Boston Children's Hospital Surgical Foundation.

Prior Presentation
Preliminary data were presented at Digestive Disease Week (May 2022; San Diego, California) as a late-breaking basic science plenary and at the International Pediatric Intestinal Failure and Rehabilitation Symposium as a top abstract (October 2022; Toronto, Ontario, Canada).

Data Availability
Raw data are provided as a downloadable excel file in the Supplementary Material.

Supplementary Materials and Methods

Preterm Piglet Delivery, Resuscitation, and Central Venous Catheter Placement

A pregnant Yorkshire sow (*Sus scrofa domesticus*) were obtained (Parson's Farm) and housed in our facility 5 days before cesarean section. The sow was induced with atropine (0.04 mg/kg), tiletamine/zolazepam (2.2 mg/kg), xylazine (1.1 mg/kg), and propofol (1 mg/kg). General anesthesia was maintained with inhaled isoflurane (1%–5%) via mask inhalation; 500 mL of whole blood was drawn from the left femoral vein into a collection bag containing citrate phosphate double dextrose solution (Haemonetics). After this, a lower midline incision was made. One horn of the uterus was exteriorized and incised with electrocautery over the back of a piglet. The piglet was delivered from the uterus, the oropharynx was suctioned, the umbilical cord was ligated and divided, and the piglet was handed off the surgical field for resuscitation. Subsequent piglets were delivered in this fashion. After all piglets were delivered, the sow was euthanized using sodium pentobarbital (110 mg/kg).

After delivery, piglets were dried, vigorously stimulated, warmed, and administered doxapram (4 mg), atropine (0.11 mg), and vitamin B12 (500 μg) via intramuscular injection. If necessary, ventilation and supplemental oxygen were provided via bag-valve mask. Epinephrine was administered if piglets developed bradycardia, and additional doxapram was given for hypoventilation. Piglets were then placed in a humified incubator at 37°C. After adequate resuscitation, piglets were induced and intubated. Single-lumen (3 Fr $\times$ 8 cm) central venous catheters (Cook Medical) were placed preferentially in the right external jugular vein. Intravenous cefazolin (20 mg/kg), flunixin (1 mg/kg), buprenorphine (0.01 mg/kg), maropitant citrate (1 mg/kg), and intramuscular iron (75 mg/kg) were administered. The piglets were returned to incubators and cohoused per animal welfare recommendations (2 piglets per incubator bay).

Total Parenteral Nutrition

TPN was initiated on DOL 1, advanced to goal over 5 days, and continued until sacrifice on DOL 15. The goal daily volume was 162 mL/kg/d; dextrose, 16 g/kg/d; amino acids, 9 g/kg/d; fat, 5.7 g/kg/d; and caloric content, 143 kcal/kg/g. The parenteral nutrition composition was based on the previously published work of Vlaardingerbroek et al,[1] with the volume decreased after the pilot cohort demonstrated intolerance of a higher dextrose infusion rate (see Supplementary Figure 1). TPN was compounded daily in a class II biosafety cabinet with sterile technique using a premixed parenteral nutrition solution (Clinimix e 8/14, Baxter), soybean oil lipid emulsion (Nutrilipid, B. Braun), intravenous multivitamins (Infuvite, Baxter), and sterile water for injection (Baxter). TPN was advanced at the following daily rate as a percentage of goal: day 1, 43%; day 2, 69%; day 3, 82%; day 4, 95%; and day 5, 100%. Piglets were monitored for signs of TPN intolerance, including hyperglycemia on ear stick blood glucose, and evidence of dehydration, such as lethargy. If there was concern for TPN intolerance, the rate of TPN was decreased to the previous rate, supplemental isotonic intravenous fluids were provided, and TPN was readvanced after normalization of glucose or activity.

Immunohistochemistry

Formalin-fixed, paraffin-embedded liver sections were stained using 3,3′-diaminobenzidine tetra hydrochloride immunohistochemistry by HistoWiz Inc using a fully automated workflow on a Bond Rx autostainer (Leica Biosystems) for αSMA (Bond epitope retrieval solution 2, 20 minutes, Leica Biosystems; primary antibody: Abcam ab5694 1:1000) and cytokeratin 7 (Bond epitope retrieval solution 1, 40 minutes, Leica Biosystems; primary antibody: Abcam ab181598 1:8000). The 3,3′-diaminobenzidine tetra hydrochloride staining was performed using the IHC Polymer Detection Kit (Leica Biosystems). Whole-slide scanning (40$\times$) was performed on an Aperio AT2 (Leica Biosystems).

Messenger RNA Sequencing and Transcriptomic Analysis

Liver tissue was collected at necropsy, flash frozen in liquid nitrogen, and stored at −80°C until analysis. mRNA-Seq was performed by Novogene Co. RNA integrity was assessed with the RNA Nano 6000 Assay kit (Agilent Technologies). All samples had an RNA integrity number (RIN) of >4 and passed the established quality thresholds. mRNA was purified using poly-T oligo-attached magnetic beads, and 150–base pair paired-end reads were generated using the NovaSeq 6000 platform (Illumina). Raw data were cleaned with removal of low-quality reads and then mapped to the Sscrofa11.1 pig genome using Hisat2 v2.0.5.[2,3] Mapped reads were assembled using StringTie v1.3.3b.[4] Read numbers for each mapped gene were calculated with featureCounts v1.5.0-p3.[5] Differentially expressed genes were determined using the DESeq2 R package 1.20.0.[6] Adjusted P values of <.05 using the Benjamini-Hochberg approach for multiple testing were used for GO and KEGG enrichment analysis using clusterProfiler. Further functional pathway analysis and investigation of upstream regulators was performed using IPA (Qiagen Inc.) using differentially expressed genes with adjusted $P < .1$ and a log2foldchange of $>|0.5|$. RNA-Seq data are filed in the National Center for Biotechnology Information Gene Expression Omnibus with the accession number GSE223347.

GPR84 Activation Assay

The activity of SEFA-6179 toward GPR84 was determined in vitro using a Hit Hunter 3′-5′-cyclic adenosine monophosphate (cAMP) assay (Eurofins DiscoverX), with embelin acting as a positive control. 3′-5′-cyclic adenosine monophosphate (cAMP) Hunter cell lines were expanded from freezer stocks according to standard procedures; cells were seeded in a total volume of 20 μL into white-walled, 384-well microplates and incubated at 37°C/5% CO_2 overnight. After overnight incubation, cells were then

treated with either SEFA-6179 or embelin at 37°C/5% CO_2 or room temperature for 60 minutes. A 10-point concentration curve from 0.001 to 100 μmol/L was constructed. Compound activity was determined via chemiluminescence using β-galactosidase as the functional reporter. Percent activity was calculated using the following formula: % activity = 100% ×x (mean relative light units [RLU] of test sample – mean RLU of vehicle control) / (mean maximum control ligand – mean RLU of vehicle control).

Peroxisome Proliferator-Activated Receptor α and Peroxisome Proliferator-Activated Receptor γ Activation Assays

The activity of SEFA-6179 toward human PPARα and PPARγ was determined in vitro using PathHunter nuclear hormone receptor cell lines (Eurofins DiscoverX) with GW7647 or troglitazone acting as respective positive controls. Nuclear hormone receptor cell lines were expanded from freezer stocks according to standard procedures; cells were seeded in a total volume of 20 μL into white-walled, 384-well microplates and incubated at 37°C/5% CO_2 overnight. After overnight incubation, cells were then treated with SEFA-6179, GW7647, or troglitazone at 37°C/5% CO_2 or room temperature for 3–16 hours. A 10-point concentration curve from 0.001 to 100 μmol/L was constructed. Compound activity was determined via chemiluminescence after the addition of PathHunter Detection reagent cocktail. Microplates were read after signal generation with a PerkinElmer Envision instrument for chemiluminescent signal detection. Percent activity was calculated using the following formula: % activity = 100% × (mean RLU of test sample – mean RLU of vehicle control) / (mean MAX control ligand – mean RLU of vehicle control).

Supplementary References

1. Vlaardingerbroek H, Ng K, Stoll B, et al. New generation lipid emulsions prevent PNALD in chronic parenterally fed preterm pigs. J Lipid Res 2014;55:466–477.
2. Warr A, Affara N, Aken B, et al. An improved pig reference genome sequence to enable pig genetics and genomics research. bioRχiv Website. Available at: https://www.biorxiv.org/content/10.1101/668921v3. Updated 2019. Accessed December 11, 2022.
3. Kim D, Paggi JM, Park C, et al. Graph-based genome alignment and genotyping with HISAT2 and HISAT-genotype. Nat Biotechnol 2019;37:907–915.
4. Pertea M, Kim D, Pertea GM, et al. Transcript-level expression analysis of RNA-seq experiments with HISAT, StringTie and Ballgown. Nat Protoc 2016;11:1650–1667.
5. Liao Y, Smyth GK, Shi W. featureCounts: an efficient general purpose program for assigning sequence reads to genomic features. Bioinformatics 2014;30:923–930.
6. Love MI, Huber W, Anders S. Moderated estimation of fold change and dispersion for RNA-seq data with DESeq2. Genome Biol 2014;15(12):550.

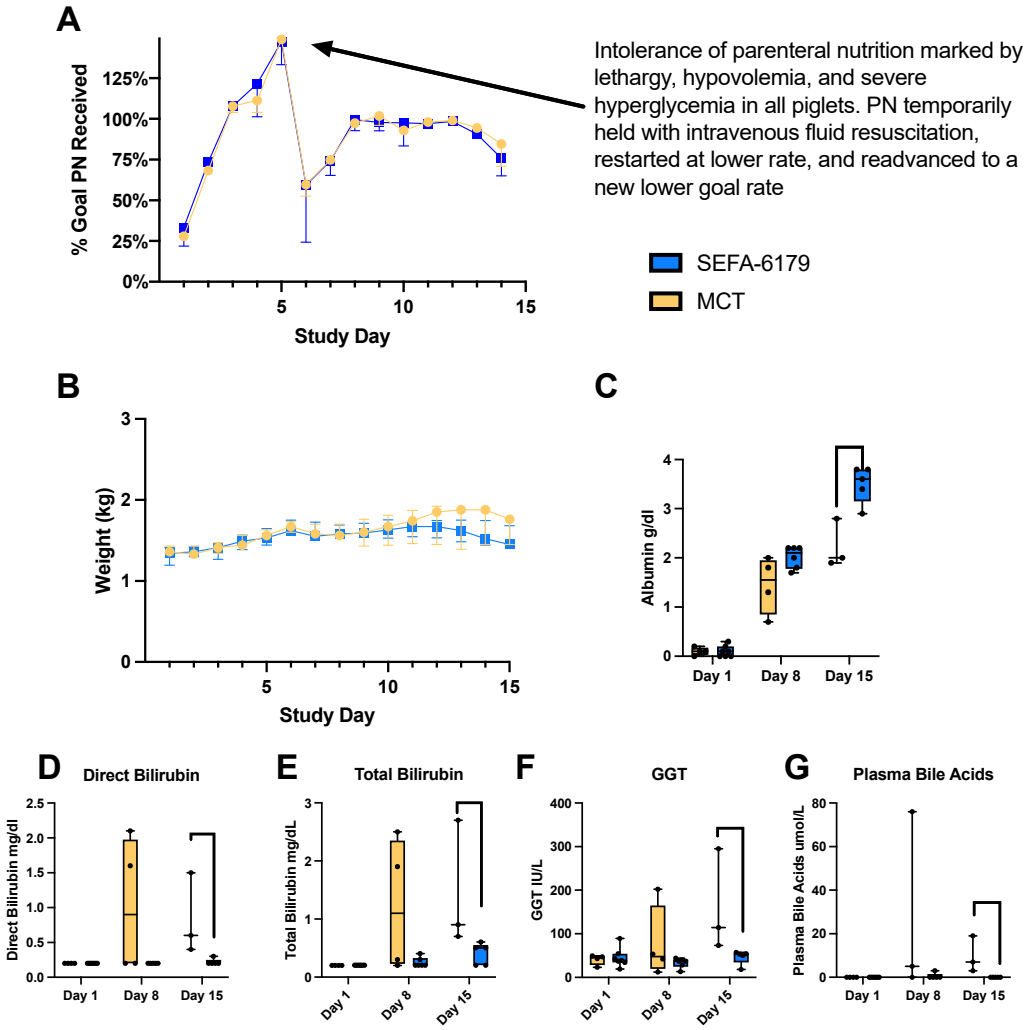

Supplementary Figure 1. A preliminary cohort of preterm piglets developed biochemical cholestasis. Piglets were delivered at 112 days gestation (4 days preterm) via cesarean section, resuscitated, and implanted with central venous catheters. Total parenteral nutrition was started as the sole source of nutrition. Piglets were randomized to daily orogastric gavage of MCT vehicle control or SEFA-6179 (24 mg/kg/d). On DOL 5, all piglets demonstrated increasing lethargy, hypovolemia, and severe hyperglycemia (600–800 mg/dL) consistent with intolerance of parenteral nutrition. (*A*) Parenteral nutrition was held, intravenous fluid resuscitation with normal saline was performed, and parenteral nutrition was restarted at a lower rate before readvancement to a lower goal rate (125 mL/kg/d, dextrose 14 g/kg/d, amino acids 8 g/kg/d, fat 5 g/kg/d) (median with interquartile range). (*B*) Piglets in each group gained similar weight from birth (median with interquartile range), and (*C*) plasma albumin increased from undetectable at birth through DOL 15. At DOL 15, albumin was higher in the SEFA-6179 group. (*D–G*) At DOL 15, piglets in the MCT group, compared to the SEFA-6179 group, demonstrated biochemical cholestasis with elevated direct bilirubin, total bilirubin, gamma glutamyl transferase, and bile acids. Comparisons of weight gain assessed was using rank-based ANCOVA, and comparison of parenteral nutrition volume was assessed by mean area under the curve and exact Wilcoxon rank sum test. Biochemical comparisons were made with exact Wilcoxon rank sum tests. Boxplots with range are shown for *C–G*. $^*P < .05$. GGT, γ-glutamyltransferase; PN, parenteral nutrition.

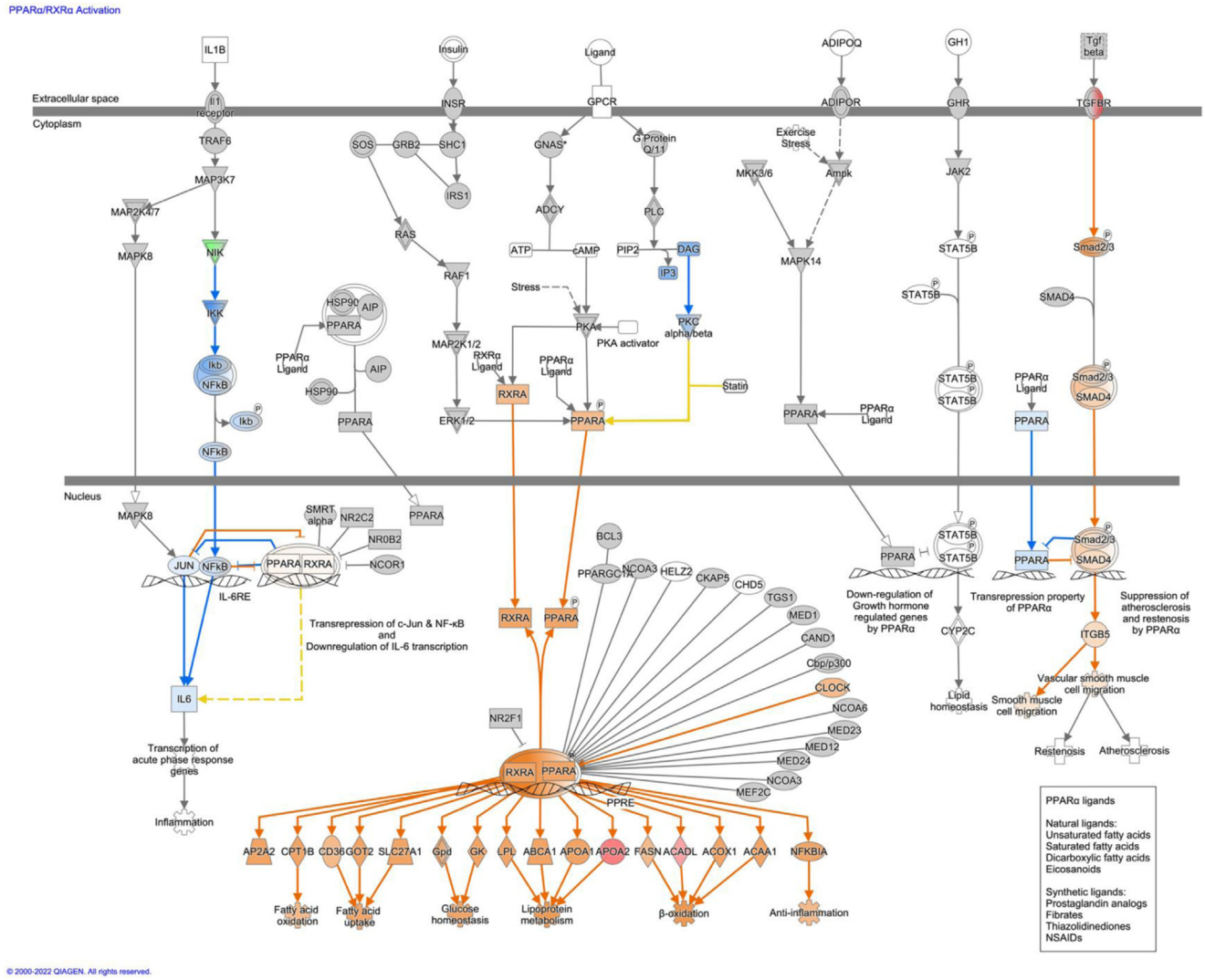

Supplementary Figure 2. Predicted activation of PPARα/RXR canonical pathway from SEFA-6179 treatment. Activation state of individual genes predicted by IPA with downstream predicted activation of fatty acid oxidation, fatty acid uptake, glucose homeostasis, lipoprotein metabolism, β-oxidation, and anti-inflammation. Green, decreased expression; red, increased expression; blue, predicted inhibition/down-regulation; orange, predicted activation/up-regulation. NSAID, nonsteroidal anti-inflammatory drug.

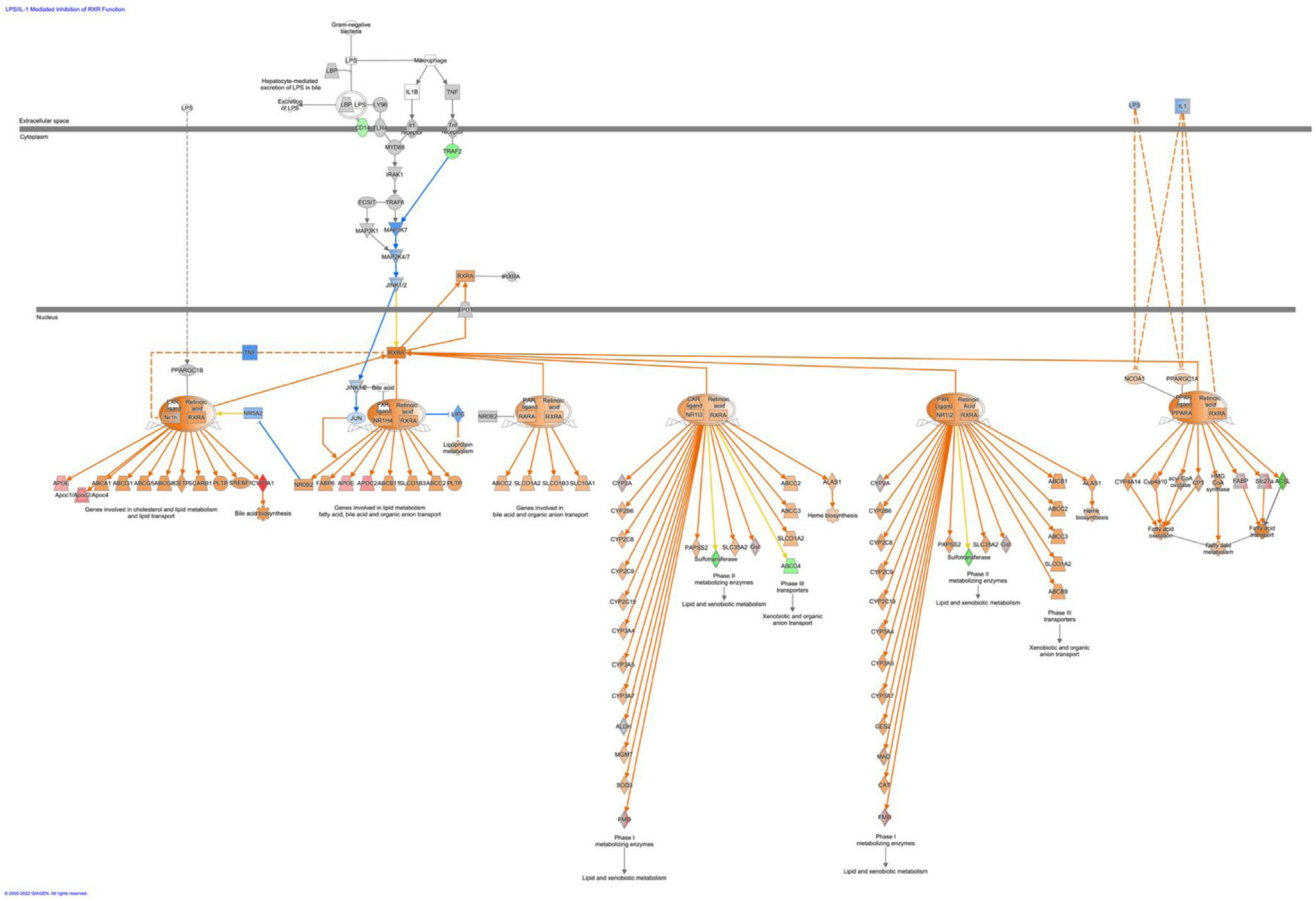

Supplementary Figure 3. Predicted inhibition of LPS/IL1–mediated inhibition of the RXR function canonical pathway from SEFA-6179 treatment. Activation state of individual genes predicted by IPA with downstream predicted activation of lipid metabolism/transport, bile acid and organic ion transport, and lipid and xenobiotic metabolism. Green, decreased expression; red, increased expression; blue, predicted inhibition/down-regulation; orange, predicted activation/up-regulation.

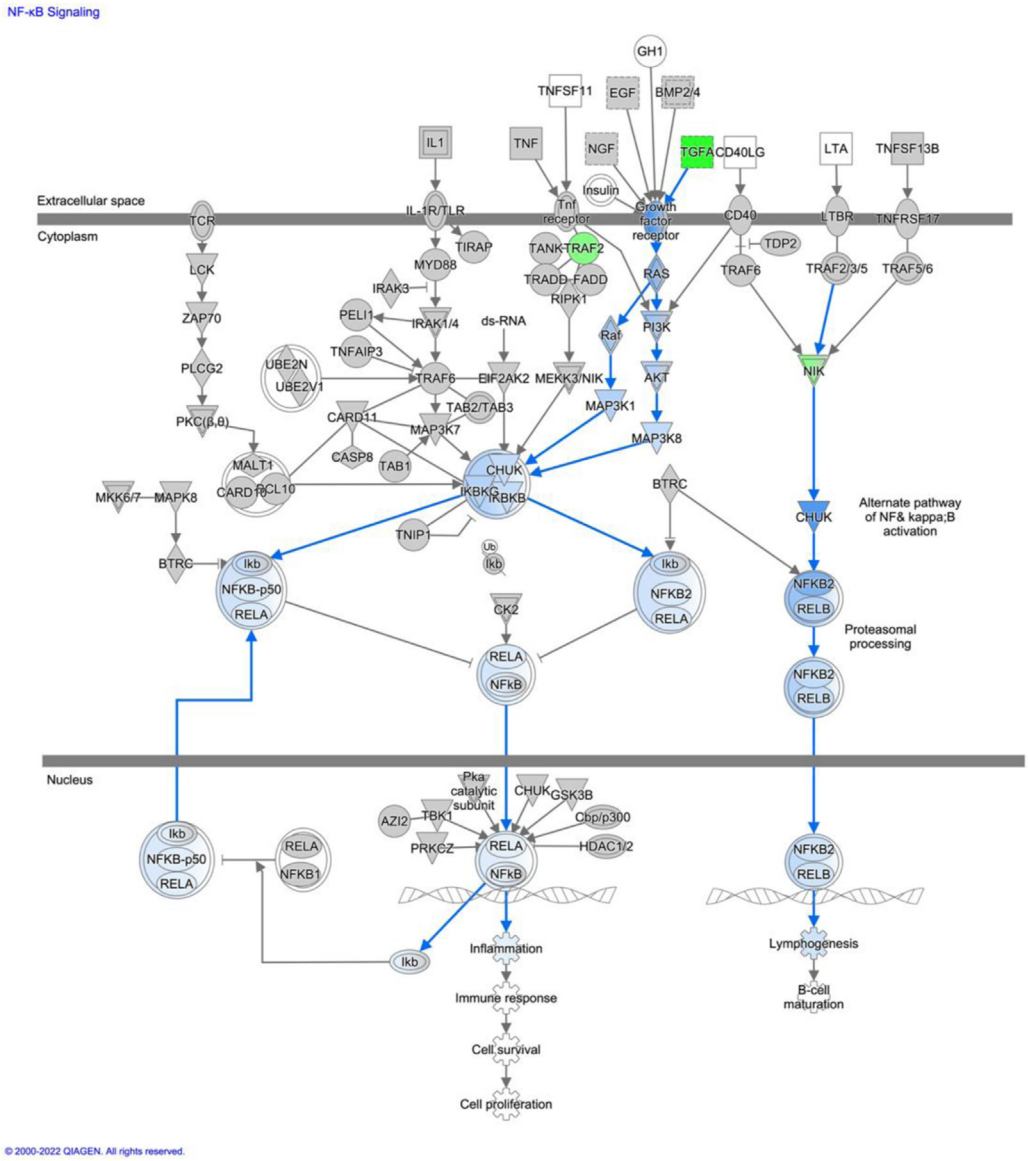

Supplementary Figure 4. Predicted inhibition of NF-kB signaling canonical pathway from SEFA-6179 treatment. Activation state of individual genes predicted by IPA with downstream predicted inhibition of inflammation. Green, decreased expression; red; increased expression; blue, predicted inhibition/down-regulation; orange, predicted activation/up-regulation.

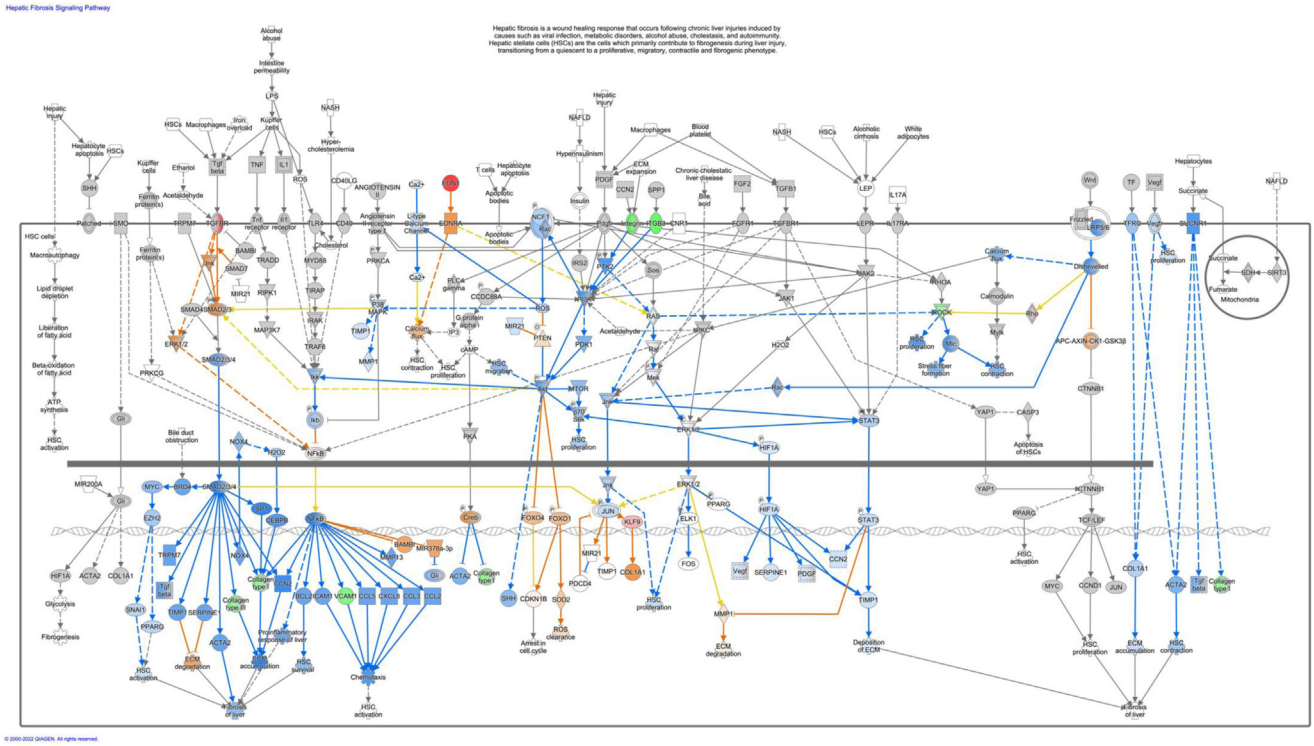

Supplementary Figure 5. Predicted inhibition of the hepatic fibrosis signaling canonical pathway from SEFA-6179 treatment. Activation state of individual genes predicted by IPA with downstream predicted activation of hepatic stellate cell activation, fibrosis of liver, chemotaxis, and deposition of extracellular matrix. Key inhibited pathways include SMAD 2/3/4, NF-κB, and JUN. Key down-regulated genes include collagen types I and III, TGF-β, and VCAM1. Green, decreased expression; red, increased expression; blue, predicted inhibition/down-regulation; orange, predicted activation/up-regulation.

Supplementary Table 1. Causes of Mortality in Preliminary Cohort of Preterm Piglets

Birth number	Sex	Group	Day of mortality	Cause of death/necropsy findings
2	M	SEFA	4	Sepsis, intestinal perforation, disseminated intravascular coagulation
7	F	MCT	14[a]	Hypoxic respiratory failure, pulmonary edema, renal failure
9	M	MCT	9	Failure to thrive, sepsis, urachal abscess with retroperitoneal/intraperitoneal extension
13	M	SEFA	9	Failure to thrive, sepsis, necrotic small bowel, intra-abdominal abscess

[a]Overall, 50% (2 of 4) of MCT piglets survived to DOL 15. Piglet 7 was euthanized on DOL 14 for hypoxic respiratory failure, but blood obtained at that time is included in the preliminary biochemical endpoints in Supplementary Figure 1. In the SEFA group, 71% (5 of 7) of SEFA-6179 (24 mg/kg/d) piglets survived to DOL 15.
F, female; M, male.

Supplementary Table 2. Causes of Mortality Identified on Necropsy

Birth number	Sex	Group	Day of mortality	Cause of death/necropsy findings
4	F	SEFA	7	Failure to thrive, acute renal failure
5	M	SEFA	5	Proximal colon perforation, sepsis
15	F	SEFA	5	Failure to thrive, acute renal failure

F, female; M, male.

Supplementary Table 3. Possible Upstream Regulators Identified in IPA Using RNA-Seq Data

Upstream regulator	Molecule type	Activation *z*-score	Target molecules in dataset
MLXIPL	Transcription regulator	4.762	KHK, RPL21, RPL23, RPL24, RPL28, RPL30, RPL31, RPL35A, RPL37, RPL37A
STK11	Kinase	4.243	ATP5MC2, ATP5MC3, ATP5MF, ATP6V0E1, BCL2L11, COX7A2, DUT, NDUFA13, NDUFA2, NDUFA3
RB1	Transcription regulator	3.357	ATP1A1, COQ7, COX17, COX4I1, COX7A2, NDUFA13, NDUFA2, NDUFA3, NDUFA4, NDUFA5
PPARGC1A	Transcription regulator	3.234	ACADM, APOC2, APOC3, COX4I1, CYP2D6, CYP7A1, CYP8B1, OLFML3, PCK1, PDK2
MYC	Transcription regulator	3.057	ACADM, CDH1, CLDN7, EGR1, EPCAM, GGT1, GLRX5, GOT1, H6PD, HP
SIGLEC8	Transmembrane receptor	3	ATP5MK, COX7A2, FAM162A, HSPE1, MIEN1, P4HA1, RPS27L, UQCC2, UQCRQ
NAMPT	Cytokine	2.449	ALDH5A1, COX4I1, COX7A2, FMO3, NDUFA4, UQCRQ
Esrra	Transcription regulator	2.236	ACADM, ATP5MC3, GOT1, NDUFA5, NDUFS3, PCK1, UQCR11
HAND2	Transcription regulator	2.224	COL1A2, COL3A1, FAP, GJA1, GJA5
GATA4	Transcription regulator	2.214	COL1A2, COL3A1, FAP, GJA1, GJA5
TBX5	Transcription regulator	2.214	COL1A2, COL3A1, FAP, GJA1, GJA5
MEF2C	Transcription regulator	2.214	COL1A2, COL3A1, FAP, GJA1, GJA5
MYOCD	Transcription regulator	2.213	COL1A2, COL3A1, FAP, GJA1, GJA5
GCG	Other	2.177	ACADL, ACADM, ACADS, PCK1, SLC25A25
IL33	Cytokine	2.168	ACTB, APOE, ATP5MK, BCL2L11, COX7A2, EMC9, FAM162A, GCHFR, HSPE1, MIEN1
PPARD	Ligand-dependent nuclear receptor	2.164	ACAA2, APOA2, APOE, CYP7A1, CYP8B1, FABP1, FAM32A, LIPG, MRC1, MYCL
FOXO1	Transcription regulator	2.152	APOC3, ATP5MC3, ATP5PF, BCL2L11, CYP7A1, HPD, MRPL34, NDUFA4, NDUFA7, PCK1
HNF4A	Transcription regulator	2.151	APOA2, APOC3, APOE, ATOX1, BET1, CAPN8, CDH1, COX17, CXADR, CYP7A1
AGT	Growth factor	–2.071	CLGN, COL1A2, COL3A1, EDN1, ITGB3, KLF15, VCAM1
PML	Transcription regulator	–2.121	ACADL, ACADM, ACADS, ACSL4, ANXA4, APOE, FABP1, TRIO
ID3	Transcription regulator	–2.236	BCL2L11, GADD45G, HOMER2, ITGB3, LMO2, NFAT5, VCAM1
MYD88	Other	–2.236	CD14, EGR1, ITPR2, MRC1, VCAM1
NR4A1	Ligand-dependent nuclear receptor	–2.353	APOE, ATP5MC3, ATP5PF, BCL2L11, COL1A2, COX7A2, NDUFA3, NDUFA6, NDUFA7, NDUFB3
TNF	Cytokine	–2.612	ACKR2, AMPD3, APOC2, CALHM6, CCN4, CD14, COL1A2, COL3A1, CYP7A1, DUSP6
KDM5A	Transcription regulator	–3.357	ATP1A1, COQ7, COX17, COX4I1, COX7A2, NDUFA13, NDUFA2, NDUFA3, NDUFA4, NDUFA5
EIF6	Translation regulator	–4.025	ATP5PF, COL3A1, COX4I1, COX7B, ETFBKMT, FABP1, MRPS21, MRPS24, NDUFA2, NDUFB7
RICTOR	Other	–5.171	ATP5MC2, ATP5MC3, ATP5MF, ATP5MG, ATP5PF, ATP6V1B1, BCL2L11, COX17, COX4I1, COX7A2

NOTE. A *z*-score of |2| was used to identify key regulators. Positive activation *z*-scores are consistent with activation of downstream pathways from the regulator, and negative activation *z*-scores are consistent with inhibition and/or down-regulation of downstream pathways.